

T_c for trapped dilute Bose gases: A second-order result

Peter Arnold and Boris Tomášik

Department of Physics, University of Virginia, P.O. Box 400714, Charlottesville, Virginia 22904-4714

(Received 7 May 2001; published 10 October 2001)

For some time, the theoretical result for the transition temperature of a dilute three-dimensional Bose gas in an arbitrarily wide harmonic trap has been known to first order in the interaction strength. We extend that result to second order. The first-order result for a gas trapped in a harmonic potential can be computed in mean-field theory (in contrast to the first-order result for a uniform gas, which cannot). We show that, at second order, perturbation theory suffices for relating the transition temperature to the chemical potential at the transition, but the chemical potential is nonperturbative at the desired order. The necessary information about the chemical potential can be extracted, however, from recent lattice simulations of uniform Bose gases.

DOI: 10.1103/PhysRevA.64.053609

PACS number(s): 03.75.Fi, 64.70.-p

I. INTRODUCTION

Consider a dilute three-dimensional gas of bosons, all identical, in an external harmonic trapping potential

$$V(\mathbf{x}) = \frac{1}{2}m(\omega_x^2 x^2 + \omega_y^2 y^2 + \omega_z^2 z^2), \quad (1.1)$$

where m is the mass of each boson. For this system to have a sharp, well-defined phase transition, we need to formally take the infinite volume limit of $\omega_x, \omega_y, \omega_z \rightarrow 0$ while keeping the central density of Bose particles finite and nonzero at the transition. As we will briefly review below, the central density \bar{n} at the transition scales as $\bar{n} \sim N^{1/2}/a_{\text{ho}}^3$, where N is the total number of Bose particles in the trap, and where

$$a_{\text{ho}}^3 \equiv \left(\frac{\hbar}{m\omega_x}\right)^{1/2} \left(\frac{\hbar}{m\omega_y}\right)^{1/2} \left(\frac{\hbar}{m\omega_z}\right)^{1/2} \quad (1.2)$$

is the volume scale of the ground-state wave function. (See also Ref. [1] for a review.) The appropriate infinite volume limit is $\omega_x, \omega_y, \omega_z \rightarrow 0$ with $N\omega_x\omega_y\omega_z$ held fixed.

At low energies, the relevant measure of the strength of interactions is the two-body scattering length a . We will assume that interactions are repulsive ($a > 0$). We will study the transition temperature T_c for Bose-Einstein condensation (BEC) of a dilute single-species gas as a function of the total number of particles N in the trap, in the infinite volume limit just discussed. One might naively anticipate there to be an expansion of the form

$$T_c(N) = T_0(N) \left[1 + c_1 \frac{a}{l} + c_2 \left(\frac{a}{l}\right)^2 + \dots \right], \quad (1.3)$$

where T_0 is the ideal-gas result and l is some characteristic length of the ideal-gas system. As we will review below, the appropriate length scale for a trapped Bose gas is the typical inter-particle separation $l \sim \bar{n}^{-1/3} \sim N^{-1/6} a_{\text{ho}}$ at the center of the trap. The coefficient c_1 of the expansion for T_c has been known for several years [2]. In this paper, we calculate the next correction. As we will discuss, this is the furthest one can go in the expansion without more information about in-

teractions than just the scattering length. We'll find that c_2 depends logarithmically on a/l ; the actual expansion is of the form

$$T_c(N) = T_0(N) \left[1 + c_1 \frac{a}{l} + \left(c_2' \ln \frac{a}{l} + c_2'' \right) \left(\frac{a}{l}\right)^2 + \dots \right], \quad (1.4)$$

and we shall calculate the constants c_2' and c_2'' . (The appearance of a related logarithm for *uniform* gases has been qualitatively discussed in Ref. [3]. For a calculation of the second-order relationship between T_c and the central density \bar{n} in an arbitrarily wide trap, which is also the relationship $T_c(n)$ for a uniform gas, see Ref. [4].)

Some aspects of the Bose-Einstein condensation phase transitions are perturbatively calculable, and others are not. In a dilute Bose gas, the physics of fluctuations associated with relatively short-distance scales is perturbative, while that associated with critical behavior on relatively long-distance scales is not. In the case of a uniform Bose gas (that is, a Bose gas in an infinite square-well potential rather than a harmonic potential) the first-order shift in T_c is sensitive to critical fluctuations and so is nonperturbative. That shift has recently been calculated using lattice simulations [5–7] and has previously been estimated in a wide variety of ways [8–14]. In contrast, the first-order shift for a gas trapped in a harmonic potential (parametrized by c_1) is calculable using perturbation theory [2]. As we shall see, the second-order logarithmic coefficient c_2' is also calculable in perturbation theory, but the constant c_2'' under the log is not. We shall calculate c_2'' by relating it to measurements that have been made in lattice simulations of the phase transition in three-dimensional O(2) field theory [7].

We should emphasize that expansions of physical quantities in a/l cease to correspond to *perturbative* expansions in a/l , once one reaches the orders we have asserted are non-perturbative. The failure of perturbation theory in describing generic second-order transitions has been known for decades. This breakdown typically manifests in perturbation theory as the appearance of infrared infinities in the coefficients of the perturbative expansion beyond a certain order.

There is a simple way to relate the problem of a Bose gas in an arbitrarily wide harmonic potential with that of a uniform Bose gas. In the infinite volume limit $\omega_x, \omega_y, \omega_z \rightarrow 0$ of the harmonic trap problem, the trapping potential becomes everywhere *locally* flat over any fixed distance scale (such as the typical interparticle spacing). Locally, the problem can then be treated as a uniform gas in the presence of an \mathbf{x} -independent potential, and an \mathbf{x} -independent potential can be absorbed into a redefinition of the chemical potential. For example, if the original chemical potential was $\bar{\mu}$, then the effective chemical potential at a position \mathbf{x} is $\bar{\mu} - V(\mathbf{x})$. For arbitrarily wide traps, the total number of particles in the system is then related to chemical potential and temperature by

$$N = \int d^3x n(T, \bar{\mu} - V(\mathbf{x})), \quad (1.5)$$

where $n(T, \mu)$ is the uniform gas result for the number density at a chemical potential μ .

In a trap, the effective chemical potential $\bar{\mu} - V(\mathbf{x})$ is highest at the center, where $V(\mathbf{x}) = 0$, and this is where the condensate first forms as the system is cooled.¹ For a uniform gas, let $\bar{\mu}_c(T)$ be the critical value μ of the chemical potential at a given temperature T . Then Eq. (1.5) becomes

$$N = \int d^3x n(T_c, \bar{\mu}_c(T_c) - V(\mathbf{x})). \quad (1.6)$$

If we knew $n(T, \mu)$ and $\bar{\mu}_c(T)$ for a uniform gas, we could then use Eq. (1.6) to solve for T_c for a gas of N particles in an arbitrarily wide trap.

In the next section, we review in more detail the physical scales of the problem and explain why, for the purposes of applying Eq. (1.6) to second order, it is adequate to use perturbation theory for the uniform gas result $n(T, \mu)$. We also explain why perturbation theory is inadequate to find the uniform gas result $\bar{\mu}_c(T)$ at second order. The second-order perturbative result for $n(T, \mu)$ can be extracted from the literature [15,16], and in Sec. III we step through the simple exercise of applying that old result to determine the relation (1.6) between N , $\bar{\mu}_c$, and T_c at second order. Then, in Sec. IV, we take on the less trivial step of showing how the second-order value of $\bar{\mu}_c(T)$ can be related to existing results from lattice simulations of O(2) scalar field theory in three dimensions. We put everything together in Sec. V, giving our final answer for the second-order term of the expansion (1.4) of T_c . In Sec. VI, we discuss the nature of yet higher-order corrections and explain why they require more knowledge of two-body scattering than just the scattering length a . In Sec. VII, we briefly discuss parametrically how wide a trap must be for our ‘‘arbitrarily wide trap limit’’ results to be valid at second order. Finally, we conclude in Sec. VIII with a brief

¹A reminder about signs: Recall that, for a uniform Bose gas, μ is negative at high temperature and increases (moves towards zero) as the system is cooled.

example of how big the second-order effects might be in a particular experimental situation. Various details and divergences are saved for appendices, including a modern field-theory rederivation and verification of the old perturbative result for $n(T, \mu)$ that we take from Huang *et al.* [15,16].

II. SCALES AND EFFECTIVE THEORIES

A. The uniform gas

Before proceeding to a Bose gas in a harmonic trapping potential, let us first review the basic scales relevant to the phase transition of a uniform gas. The generic condition that the gas is dilute is that the two-particle scattering length a be small compared to the typical interparticle separation $l \sim n^{-1/3}$, where n is the number density. The Bose-Einstein condensation phase transition occurs when the typical de Broglie wavelength

$$\lambda \equiv \hbar \sqrt{2\pi\beta/m} \quad (2.1)$$

becomes of the order of the interparticle separation l . Then $a \ll \lambda \sim n^{-1/3}$.

At the phase transition, the interaction can be treated perturbatively for analyzing short-distance physics but, as with most second-order phase transitions, interactions cannot be treated perturbatively for analyzing long-distance physics. A distance scale that will be of interest is the dividing line between these two regimes. As we shall review below, this scale is $\lambda^2/a \sim n^{-2/3}/a$. At the transition, there is then a hierarchy $\lambda^2/a \gg \lambda \gg a$ of physically relevant distance scales for a dilute Bose gas.

We will now briefly review the description of the dilute Bose gas system in terms of effective-field theories, and we will then turn to the effective-field theory description relevant to the long-distance physics at the critical point [12]. This will provide a clean way to review the origin of the nonperturbative scale λ^2/a , and we will need to make use of such effective theories later in our discussion of the critical chemical potential $\bar{\mu}_c(T)$ for a uniform gas.

B. The action

It is well known that, at distance scales large compared to the scattering length a , an appropriate effective theory for a dilute Bose gas is the second-quantized Schrödinger equation, together with a chemical potential μ that couples to particle number density $\psi^* \psi$, and a $|\psi|^4$ contact interaction that reproduces low-energy scattering [1]. The corresponding Lagrangian is

$$\mathcal{L} = \psi^* \left(i\hbar \partial_t + \frac{\hbar^2}{2m} \nabla^2 + \mu - V(\mathbf{x}) \right) \psi - \frac{2\pi\hbar^2 a}{m} (\psi^* \psi)^2. \quad (2.2)$$

The identification of the coefficient of the $(\psi^* \psi)^2$ interaction with $2\pi\hbar^2 a/m$ is technically only valid at leading order in the interaction strength but, as we will review later, does not change at second order if one uses dimensional regularization [17]. We'll also later discuss (in Sec. VI) the size of corrections to the effective theory due, for instance, to energy

dependence of the cross-section or three-body interactions. It will turn out that such corrections can be ignored for the purpose of computing T_c to second order.

To study Eq. (2.2) at finite temperature, we apply the standard imaginary time formalism, so that t becomes $-i\tau$ and imaginary time τ is periodic with period $\hbar\beta = \hbar/k_B T$. The imaginary-time action is then

$$S_I = \int_0^{\hbar\beta} d\tau \int d^3x \left[\psi^* \left(\hbar \partial_\tau - \frac{\hbar^2}{2m} \nabla^2 - \mu + V(\mathbf{x}) \right) \psi + \frac{2\pi\hbar^2 a}{m} (\psi^* \psi)^2 \right]. \quad (2.3)$$

As usual, the field ψ can be decomposed into imaginary-time frequency modes with Matsubara frequencies $\omega_n = 2\pi n/\hbar\beta$.

C. Nonperturbative physics in the uniform gas

We will now specialize the above mentioned to the uniform gas case $V(\mathbf{x})=0$ and will discuss the system at or close to the critical point. For distances large compared to the thermal wavelength (2.1) and sufficiently near the transition so that $|\mu| \ll T$, the nonzero Matsubara frequencies decouple from the dynamics, leaving behind an effective theory of only the zero-frequency modes ψ_0 , with the action becoming

$$\hbar^{-1} S_I \rightarrow \beta \int d^3x \left[\psi_0^* \left(-\frac{\hbar^2}{2m} \nabla^2 - \mu_{\text{eff}} \right) \psi_0 + \frac{2\pi\hbar^2 a}{m} (\psi_0^* \psi_0)^2 \right], \quad (2.4)$$

up to corrections that again, as we will discuss later (in Sec. VI), do not affect T_c at second order. Equation (2.4) can be interpreted, if desired, as the βH of a classical three-dimensional field theory.

Finally, it is convenient to rewrite $\psi_0 = \phi \sqrt{4\pi}/\lambda$ so that the effective action becomes a conventionally normalized U(1) field theory of a complex field ϕ :

$$S = \int d^3x \left[(\nabla \phi)^* \cdot (\nabla \phi) + r \phi^* \phi + \frac{u}{6} (\phi^* \phi)^2 \right], \quad (2.5)$$

where

$$u = \frac{96\pi^2 a}{\lambda^2}. \quad (2.6)$$

We will henceforth refer to this effective theory as the “three-dimensional” effective theory, while referring to the original imaginary time theory (2.3) as the “3+1-dimensional theory” (for three space plus one time dimension). By writing $\phi = (\phi_1 + i\phi_2)/\sqrt{2}$, the three-dimensional effective theory may equivalently be interpreted as an O(2) theory of two real fields with interaction $(u/4!)(\phi_1^2 + \phi_2^2)^2$. The relationship of r to the chemical potential μ and other parameters of the original theory is a little more subtle, be-

cause the $\phi^* \phi$ interaction is associated with an ultraviolet (UV) divergence of the three-dimensional theory that has to be renormalized. We will discuss this relationship in detail when we analyze $\bar{\mu}_c(T)$ in Sec. IV. For the moment, these details are unimportant.

There will be a line in the (μ, T) plane that corresponds to the Bose-Einstein condensation phase transition. In the long-distance effective theory (2.5), that line will correspond to a line in the (r, u) plane. If we think of this line as determining r in terms of u , then the only physical scale in the problem of studying this effective theory at the transition is u . By dimensional analysis, the distance scale of nonperturbative physics is therefore $1/u \sim \lambda^2/a$, as asserted earlier.

It will be useful to understand how far away from the transition one needs to go, as measured by $\bar{\mu}_c - \mu$ at $T = T_c$, in order for the physics on *all* scales to be perturbative. This will happen when the correlation length ξ is small compared to the scale $1/u \sim \lambda^2/a$ of nonperturbative physics. We can determine this condition on ξ with a perturbative analysis. In fact, it is sufficient to consider a simple Gaussian (i.e., tree-level) approximation, where μ_{eff} in the effective three-dimensional theory (2.4) is naively taken to be μ , corresponding to $r = -2m\mu/\hbar^2$ in the rescaled effective theory (2.5). In Gaussian approximation, $\bar{\mu}_c = 0$. The correlation length, in the Gaussian approximation, is $\xi \sim r^{-1/2}$, and so the condition $\xi \ll 1/u$ becomes

$$\bar{\mu}_c - \mu \gg \frac{\hbar^2 u^2}{m} \sim \frac{\hbar^2 a^2}{m\lambda^4}. \quad (2.7)$$

(An equivalent condition was discussed in the original work [2] on the first-order result for T_c in a trap.) We’ll see later, in our more thorough discussion of the relationship between r and μ in Sec. IV, that corrections to the Gaussian approximation do not change this conclusion.

Finally, note that, by dimensional analysis, the nonperturbative contribution to the critical value of r in the three-dimensional O(2) effective theory (2.5) must be of order u^2 . The Gaussian approximation’s identification of r with $-2m\mu/\hbar^2$ then suggests that the nonperturbative contribution to the critical value $\bar{\mu}_c$ is of order $\hbar^2 u^2/m$, which is second order in a . As we will see in Sec. IV, this conclusion is correct. This is the reason that, in order to calculate T_c to second order, we must account for nonperturbative physics in the determination of $\bar{\mu}_c$.

D. Gas in a harmonic trap

Now we turn to reviewing scales in a harmonic trap. One of the main points of this exercise will be to determine the size of the region (at the transition) where the physics is nonperturbative, relative to the size of the trapped gas cloud as a whole. This will allow us to determine to what order one can use perturbative calculations to relate N , T , and μ via Eq. (1.5).

For simplicity, we’ll assume in this discussion that $\omega_x \sim \omega_y \sim \omega_z$. The relevant distance scales for a dilute Bose gas in an arbitrarily wide harmonic trap, at the transition, are

TABLE I. Distance scales for a dilute Bose gas in an arbitrarily wide harmonic trap at the phase transition. The scales are ranked in ascending order. Entries should be interpreted as representing orders of magnitude (parametric dependence) and not as precise definitions and equalities. The first column gives our notation for each scale. The third column shows how the scales depend on the “experimental” parameters a , m , N , and ω , where $a_{\text{ho}} \equiv (\hbar/m\omega)^{1/2}$. The last column shows a simple rewriting that makes the ordering of scales clear, given that our assumed limits can be phrased as a fixed, $a \ll l$ (diluteness), and l fixed with $N \rightarrow \infty$ (arbitrarily wide trap).

a	Scattering length	a	a
$l \sim \bar{n}^{-1/3} \sim \lambda$	interparticle separation at trap center; thermal wavelength	$N^{-1/6} a_{\text{ho}}$	l
$1/u$	smallest wavelength of nonperturbative fluctuations near center of trap	$N^{-1/3} a_{\text{ho}}^2/a$	l^2/a
a_{ho}	size of the ground state (condensate)	a_{ho}	$N^{1/6} l$
R_{np}	size of nonperturbative region	$N^{1/3} a$	$N^{1/3} a$
R_{cloud}	size of entire gas cloud	$N^{1/6} a_{\text{ho}}$	$N^{1/3} l$

summarized in Table I in ascending order. Most of this is just review of simple, standard results [1], except for the scales of nonperturbative physics in a harmonic trap, which we have not seen clearly discussed before.

First, let us review the size and density of the cloud of Bose particles at the phase transition. As we will reproduce below, *most* of the particles in the trap are in the classical regime, and we can use the classical equipartition theorem to find the width R_{cloud} of the cloud; $\frac{1}{2}m\omega^2 x^2 \sim \frac{1}{2}k_B T$ yields $R_{\text{cloud}} \sim (\beta m \omega^2)^{-1/2}$. The central density of particles is then of order $\bar{n} \sim N/R_{\text{cloud}}^3 \sim N(\beta m \omega^2)^{3/2}$, and the separation of particles at the center of the trap is of order of $l \sim \bar{n}^{-1/3} \sim N^{-1/3}(\beta m \omega^2)^{-1/2}$. The phase transition occurs when this separation is of order the thermal wavelength (2.1), giving $k_B T \sim N^{1/3} \hbar \omega$, and so $l \sim \bar{n}^{-1/3} \sim \lambda \sim N^{-1/6} a_{\text{ho}}$, as claimed in Table I. The fact that $k_B T \sim N^{1/3} \hbar \omega \gg \hbar \omega$ in our wide trap limit (which has $N \rightarrow \infty$) justifies the previous assertion that, at the phase transition, most particles in the cloud can be treated classically.

Now let us analyze the size of the region in which physics is nonperturbative at the transition. In our review of the uniform gas, we saw that physics becomes completely perturbative when $\bar{\mu}_c - \mu \gg \hbar^2 a^2 / m \lambda^4$. In an arbitrarily wide trap, the effective value of μ is $\bar{\mu} - \frac{1}{2}m\omega^2 x^2$. The condition for the existence of nonperturbative physics at the transition is then $\frac{1}{2}m\omega^2 x^2 \lesssim \hbar^2 a^2 / m \lambda^4$, and the width of the nonperturbative region is $R_{\text{np}} \sim \hbar a / m \omega \lambda^2 \sim N^{1/3} a$. Note that, even within this “nonperturbative” region, fluctuations with small wavelengths ($\ll 1/u$) are still perturbative.

The relative volume of the nonperturbative region to the volume of the entire gas cloud is $(R_{\text{np}}/R_{\text{cloud}})^3 \sim (a/l)^3$. This means that nonperturbative contributions to the relation $N = \int d^3x n(T, \bar{\mu} - V(\mathbf{x}))$ between N , T , and $\bar{\mu}$ are suppressed by more than three powers of $(a/l)^3$. It is *more* than three powers because, even in the relatively small nonperturbative regime, the dominant contribution to the density comes from typical particles, whose wavelengths are of the order of the thermal wavelength $\lambda \gg 1/u$, which can be treated perturbatively. This makes the total suppression $(a/l)^4$. In any case,

the conclusion is that there is no obstacle at second order in a/l to using perturbation theory to derive the relationship between N , T , and $\bar{\mu}$.

III. $n(T, \mu)$ FOR A UNIFORM GAS AND ITS APPLICATION

The second-order perturbative result for $n(T, \mu)$ can be easily extracted from an old second-order result of Huang *et al.* [15,16] for the pressure of a uniform hard-sphere gas:

$$\begin{aligned}
 P = \frac{k_B T}{\lambda^3} & \left\{ \text{Li}_{5/2}(z) - \frac{2a}{\lambda} [\text{Li}_{3/2}(z)]^2 \right. \\
 & + 8 \left(\frac{a}{\lambda} \right)^2 \left([\text{Li}_{3/2}(z)]^2 \text{Li}_{1/2}(z) \right. \\
 & \left. \left. + \sum_{i=1}^{\infty} \sum_{j=1}^{\infty} \sum_{k=1}^{\infty} \frac{z^{i+j+k}}{(i+k)(j+k)(ijk)^{1/2}} \right) + \dots \right\},
 \end{aligned} \tag{3.1}$$

where

$$z = e^{\beta \mu} \tag{3.2}$$

is the fugacity. Li_n is the polylogarithm function, which for our purposes can be considered as defined in terms of its series representation,

$$\text{Li}_n(z) = \sum_{s=1}^{\infty} \frac{z^s}{s^n}. \tag{3.3}$$

We have independently rederived and verified this result for the pressure. For the sake of any readers who might find a derivation in the language of field theory [based on the Lagrangian (2.2)] a useful supplement to the original, we give the derivation in Appendix A. In the language of the imaginary-time field theory (2.3), the perturbative Feynman diagrams, which correspond to the first- and second-order terms in the pressure (3.1) are shown in Fig. 1.

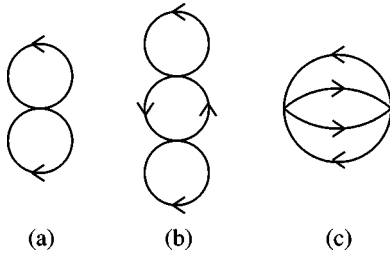


FIG. 1. Perturbative Feynman diagrams contributing to the pressure P at (a) first order and (b) and (c) second order. Diagram (b) corresponds to the first $(a/\lambda)^2$ term in Eq. (3.1) and diagram (c) to the second.

We now obtain n as $\partial P/\partial\mu$

$$n = \frac{1}{\lambda^3} \left\{ \sum_i \frac{z^i}{i^{3/2}} - \frac{2a}{\lambda} \sum_{ij} \frac{(i+j)z^{i+j}}{(ij)^{3/2}} + 8 \left(\frac{a}{\lambda}\right)^2 \sum_{ijk} (i+j+k) \times z^{i+j+k} \left[\frac{1}{(ij)^{3/2}k^{1/2}} + \frac{1}{(i+k)(j+k)(ijk)^{1/2}} \right] + \dots \right\}. \quad (3.4)$$

Here and henceforth, indices of sums (i, j, k) implicitly run from 1 to infinity. (Most of the terms above could be written in terms of polylogarithms, but the form shown is more convenient for the next step.) We emphasize that this is a perturbative expansion and is valid only in contexts where perturbation theory is applicable.² In field theory language, the above result for n corresponds to the diagrams of Fig. 2.

Now, use $\mu = \bar{\mu} - V(\mathbf{x})$ and integrate over \mathbf{x} , as in Eq. (1.5). For the harmonic potential (1.1), the integrals are simple Gaussian integrals, giving

$$N = \left(\frac{k_B T}{\hbar \omega_{\text{ho}}}\right)^3 \left\{ \sum_i \frac{\bar{z}^i}{i^3} - \frac{2a}{\lambda} \sum_{ij} \frac{\bar{z}^{i+j}}{(ij)^{3/2}(i+j)^{1/2}} + 8 \left(\frac{a}{\lambda}\right)^2 \sum_{ijk} \frac{\bar{z}^{i+j+k}}{(i+j+k)^{1/2}} \left[\frac{1}{(ij)^{3/2}k^{1/2}} + \frac{1}{(i+k)(j+k)(ijk)^{1/2}} \right] + \dots \right\}, \quad (3.5)$$

where $\bar{z} \equiv e^{\beta \bar{\mu}}$ and

$$\omega_{\text{ho}} \equiv (\omega_x \omega_y \omega_z)^{1/3} \quad (3.6)$$

is the geometric mean of the trap frequencies.

In Sec. IV, we will discuss the expansion

²The same expansion was incorrectly applied in Ref. [18] to the problem of the first-order correction to T_c for a uniform gas—a problem where perturbation theory breaks down.

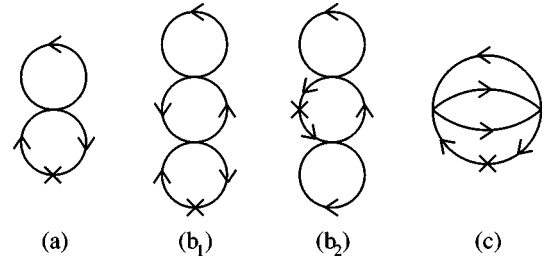


FIG. 2. Perturbative Feynman diagrams contributing to the number density $n = \langle \psi^* \psi \rangle$ at (a) first order and (b₁, b₂, and b₃) second order. The cross corresponds to an insertion of the operator $\psi^* \psi$, whose expectation is being taken.

$$\bar{\mu}_c = \left[\bar{\mu}_c^{(1)} \frac{a}{\lambda} + \bar{\mu}_c^{(2)} \left(\frac{a}{\lambda}\right)^2 + \dots \right] k_B T \quad (3.7)$$

of the critical value of $\bar{\mu}$ in powers of a . The ideal-gas result is $\bar{\mu}_c = 0$. Recall from previous discussions that the second-order term $\bar{\mu}_c^{(2)}$ is not perturbatively calculable.³ We will later see that the second-order coefficient $\bar{\mu}_c^{(2)}$ contains a logarithm,

$$\bar{\mu}_c^{(2)} = A \ln \frac{a}{\lambda} + B, \quad (3.8)$$

and that the coefficient A of the logarithm is perturbatively calculable, while B is not.

³For those readers who like to think in terms of Feynman diagrams, there is a hand-waving, heuristic argument to see why there is a nonperturbative $\mathcal{O}(a^2)$ contribution to $\bar{\mu}_c$. The first-order contribution, given by the first diagram of Fig. 3, contributes $\mathcal{O}(a)$ to μ . Since this diagram is momentum independent, it can be absorbed into a renormalization of μ , so that one need not consider higher-order diagrams that contain it as a subdiagram (a point relevant to the discussion of divergencies at higher orders). At the transition, the second diagram of Fig. 3 contributes $\mathcal{O}(a^2)$ times a logarithmic infrared (IR) divergence, arising from the contribution where both loop frequencies are zero and the two loop momenta simultaneously approach zero. Three-loop contributions turn out to produce $\mathcal{O}(a^3)$ times linear IR divergencies, four loops produce quadratic divergencies, and so forth. Suppose we heuristically cut off these infrared divergencies at a momentum scale Λ_{IR} . The perturbation series then turns out to look like $\beta \bar{\mu}_c = \mathcal{O}(a/\lambda) + \mathcal{O}(a^2/\lambda^2) + \mathcal{O}(a^3/\lambda^4 \Lambda_{\text{IR}}) + \mathcal{O}(a^4/\lambda^6 \Lambda_{\text{IR}}^2) + \dots$, where we have ignored logarithms such as $\ln(\lambda \Lambda_{\text{IR}})$. Imagine starting Λ_{IR} at some high value and then lowering it. The usefulness of the perturbative expansion will break down once we get to $\Lambda_{\text{IR}} \sim a/\lambda^2$, which is just the nonperturbative scale u discussed earlier. For this Λ_{IR} , all the terms in the series after the first become the same order, which is $\mathcal{O}(a^2/\lambda^2)$. This suggests that this is the order of a nonperturbative contribution to $\beta \bar{\mu}_c$. For a clean argument, however, one should instead refer to the analysis in the text.

In any case, we would like to insert the expansion (3.7) for $\bar{\mu}_c$ into the expansion (3.5) for N . The problem is a little more complicated than simply Taylor series expanding the individual terms of the sums of Eq. (3.5) in $\bar{\mu}$, because such a procedure would lead to unregulated infrared logarithmic divergencies at second order. We derive the small $\bar{\mu}$ expansion of Eq. (3.5) in detail in Appendix B, with the result

$$\begin{aligned}
 N = & \left(\frac{k_B T}{\hbar \omega_{\text{ho}}} \right)^3 \left\{ \zeta(3) + \frac{a}{\lambda} \left[\zeta(2) \bar{\mu}^{(1)} - 2 \sum_{ij} \frac{1}{i^{3/2} j^{3/2} (i+j)^{1/2}} \right] \right. \\
 & + \left(\frac{a}{\lambda} \right)^2 \left[\frac{3}{4} [\bar{\mu}^{(1)}]^2 + \zeta(2) \bar{\mu}^{(2)} \right. \\
 & - 2 \bar{\mu}^{(1)} \sum_{ij} \frac{(i+j)^{1/2} - i^{1/2} - j^{1/2}}{i^{3/2} j^{3/2}} - 4 \zeta\left(\frac{3}{2}\right) \bar{\mu}^{(1)} \\
 & + 8 \sum_{ijk} \frac{1}{(ij)^{3/2} k^{1/2}} \left(\frac{1}{(i+j+k)^{1/2}} \right. \\
 & \left. \left. + \frac{ij}{(i+k)(j+k)(i+j+k)^{1/2}} - \frac{1}{k^{1/2}} \right) \right] \\
 & \left. - \frac{1}{2} \left(\frac{a}{\lambda} \right)^2 (\bar{\mu}^{(1)} - 4 \zeta\left(\frac{3}{2}\right))^2 \ln \left(- \frac{\bar{\mu}^{(1)} a}{\lambda} \right) + O \left(\frac{a}{\lambda} \right)^3 \right\}. \quad (3.9)
 \end{aligned}$$

The logarithmic term at the end is the manifestation of the infrared logarithm just mentioned. In fact, at the critical point, the coefficient of this logarithm vanishes because

$$\bar{\mu}_c^{(1)} = 4 \zeta\left(\frac{3}{2}\right). \quad (3.10)$$

A diagrammatic interpretation of why the logarithm vanishes is given at the end of Appendix B. The first-order result (3.10) for $\bar{\mu}_c^{(1)}$ can be derived using mean-field theory, and a discussion in the context of trapped Bose gases may be found in the original first-order derivation of T_c [2]. We will rederive it in the next section, along with the second-order coefficient $\bar{\mu}_c^{(2)}$. For the moment, though, let us use the known first-order result (3.10) to solve for T_c in terms of $\bar{\mu}_c^{(2)}$. Inverting Eq. (3.9) gives

$$T_c = T_0 \left[1 + c_1 \frac{a}{\lambda_0} + c_2 \left(\frac{a}{\lambda_0} \right)^2 + O \left(\frac{a}{\lambda_0} \right)^3 \right], \quad (3.11a)$$

$$\begin{aligned}
 c_1 = & \frac{2}{3 \zeta(3)} \left[\sum_{ij} \frac{1}{i^{3/2} j^{3/2} (i+j)^{1/2}} - 2 \zeta(2) \zeta\left(\frac{3}{2}\right) \right] \\
 \simeq & -3.426032, \quad (3.11b)
 \end{aligned}$$

$$c_2 = C_2 - \frac{\zeta(2)}{3 \zeta(3)} \bar{\mu}_c^{(2)}, \quad (3.11c)$$

$$\begin{aligned}
 C_2 = & \frac{5}{2} c_1^2 + \frac{4}{3 \zeta(3)} \left[\zeta\left(\frac{3}{2}\right)^2 + 2 \zeta\left(\frac{3}{2}\right) \sum_{ij} \frac{(i+j)^{1/2} - i^{1/2} - j^{1/2}}{i^{3/2} j^{3/2}} \right. \\
 & - 2 \sum_{ijk} \frac{1}{(ij)^{3/2} k^{1/2}} \left(\frac{1}{(i+j+k)^{1/2}} \right. \\
 & \left. \left. + \frac{ij}{(i+k)(j+k)(i+j+k)^{1/2}} - \frac{1}{k^{1/2}} \right) \right] \simeq 21.4, \quad (3.12)
 \end{aligned}$$

where

$$T_0 = \left(\frac{N}{\zeta(3)} \right)^{1/3} \frac{\hbar \omega_{\text{ho}}}{k_B} \quad (3.13)$$

is the ideal-gas result and

$$\lambda_0 = \sqrt{\frac{2 \pi \hbar^2}{m k_B T_0}} = \sqrt{2 \pi} \left(\frac{N}{\zeta(3)} \right)^{-1/6} a_{\text{ho}} \quad (3.14)$$

is the corresponding thermal wavelength. The first-order result is the same as that found in Ref. [2].⁴ Results for the individual sums appearing above are listed in Appendix C.

IV. $\bar{\mu}_c(T)$ FOR A UNIFORM GAS

A. Overview

We'll now address how to relate the chemical potential μ appearing in the original (3+1)-dimensional theory (2.2) to the parameter r of the effective three-dimensional theory (2.5). The critical value r_c of r can be extracted from lattice simulations of the latter theory [7], which will then allow us to determine the critical value $\bar{\mu}_c(T)$ of μ .

Effective theories, such as the three-dimensional O(2) model, have long been used to describe long-distance physics at second-order phase transitions. Such use of effective theories is often restricted to studies of universal quantities, such as critical exponents, because the relationship between the parameters of the effective theory and a more fundamental description of the system cannot be computed systematically. The situation is quite different for dilute Bose gases near the phase transition; the short distance scale λ at which the long-distance three-dimensional effective theory description (2.5) breaks down is a scale at which the physics is *perturbative* (since $\lambda \ll 1/u$). One may therefore perform a perturbative calculation to relate r to μ , even though the long-distance physics at the transition is nonperturbative.

Such perturbative matching of the parameters of effective theories with underlying physics has a long history in field theory. It has been applied in a number of problems, includ-

⁴The sum in Eq. (3.11b) is expressed in a slightly different form than in Ref. [2]. The relation is that

$$\sum_{ij} \frac{1}{i^{3/2} j^{3/2} (i+j)^{1/2}} = \sum_{ij} \frac{(i+j)}{i^{3/2} j^{3/2} (i+j)^{3/2}} = 2 \sum_{ij} \frac{1}{i^{3/2} j^{1/2} (i+j)^{3/2}},$$

where we have used $i \leftrightarrow j$ in the last step.

TABLE II. Feynman rules, appropriate for a matching calculation in a uniform Bose gas, for the original 3+1 dimensional theory (2.3) of ψ and the effective three-dimensional theory (2.5) of ϕ . We have set $\hbar = k_B = 1$. The variable k_0 represent the Matsubara frequency of the field, while $\omega_{\mathbf{k}} \equiv k^2/2m$. At finite temperature, loop frequencies l_0 are summed over the discrete values $l_0 = 2\pi nT$ with n any integer. In dimensional regularization with the $\overline{\text{MS}}$ renormalization scheme, a factor of $M^\epsilon = (e^{\gamma_E/2} \overline{M} / \sqrt{4\pi})^\epsilon$ should also be associated with each four-point vertex but has not been explicitly shown above.

	(3+1)-dimensional theory of ψ	3-dimensional theory of ϕ
	$\frac{1}{ik_0 + \omega_{\mathbf{k}}}$	$\frac{1}{k^2}$
	$+\mu$	$-r$
	$-\frac{8\pi a}{m}$	$-\frac{2u}{3}$

ing lattice field theory [19], Bose condensates at zero temperature [20], relativistic corrections to nonrelativistic QED [21], heavy quark physics [22], ultrarelativistic plasmas [23], and nonrelativistic plasma physics [24]. For a general discussion, see also Ref. [25]. The basic idea is to formally compute, in perturbation theory, some number of infrared physical quantities in both the effective theory and the more fundamental theory. By equating the results from the two theories, one can then solve for the parameters of the effective theory (to the order desired).

The perturbative computations are performed using any convenient infrared regulator (though it must be the same regulator in both theories). The perturbation series for various physical quantities will be badly behaved if one removes the infrared regulator since, in our case at least, the infrared physics is nonperturbative. But this bad infrared behavior will cancel out in the perturbation series derived for the parameters of the effective theory, and so one may safely remove the infrared regulator at the end of the matching calculation. This is a reflection of the fact that the difference between the effective theory and underlying theory has to do with short-distance physics, and short-distance physics is perturbative (in the cases where perturbative matching is applicable).

The relevant distance scale of physics for the matching calculation is the short-distance scale λ where the three-dimensional O(2) theory breaks down. The corresponding energy scale is therefore of order $\hbar^2/m\lambda^2 \sim k_B T$, which is simply the typical energy of particles in the gas. This scale is large compared to the size of the chemical potential at the transition (3.7), which is of order $(a/\lambda)k_B T$. Therefore, for the purpose of doing a matching calculation, the chemical potential μ may be treated as a perturbation. In combination with the use of dimensional regularization, this turns out to be very convenient computationally.

With μ treated perturbatively, the imaginary-time Feynman rules for the original 3+1 dimensional action (2.3) are shown, for reference, in Table II. The analogous rules for the three-dimensional O(2) effective theory are also shown. When discussing the evaluation of Feynman diagrams, we will always set $\hbar = k_B = 1$ in order to avoid cluttering up equations and discussions of conventions. We have special-

ized to the case of a uniform gas by taking $V(\mathbf{x})=0$, and we've introduced the shorthand

$$\omega_{\mathbf{k}} \equiv \frac{k^2}{2m}. \tag{4.1}$$

We will use the notation k_0, l_0, p_0, \dots to designate the Matsubara (imaginary time) frequencies associated with propagators with momenta $\mathbf{k}, \mathbf{l}, \mathbf{p}, \dots$.

In our case, the short-distance length scale Λ^{-1} at which the three-dimensional theory breaks down is of order $n^{-1/3} \sim \lambda$, as we have discussed before. In principal, a long-distance effective theory can correctly describe physics at an infrared wavelength scale $k \leq \Lambda$ to any desired order in k/Λ . However, as one pushes the description to higher and higher powers of k/Λ , one must add more and more corrections to the action of the effective theory, in the form of interactions that are more and more infrared irrelevant (in the sense of the renormalization group)—that is, interactions with higher scaling dimension. In our case, the long-distance physics scale of interest is the nonperturbative scale $1/u$, and powers of k/Λ translate into powers of our expansion parameter $u\lambda \sim a/\lambda \ll 1$. We shall discuss later why including such corrections, such as a $|\phi^* \nabla \phi|^2$ term in the effective Lagrangian, would in particular not affect T_c at second order. [We will also give a similar discussion of $(\phi^* \phi)^3$, which is a marginal operator in three dimensions.] For now, though, we shall simply ignore the issue and push ahead with the matching calculation.

The action for a given effective theory can be written in a variety of equivalent ways by making field redefinitions, such as $\phi \rightarrow c\phi$ or $\phi \rightarrow (1 + \epsilon \nabla^2 + \dots)\phi$, etc. Our convention shall be to insist that the fields of the three-dimensional and 3+1 dimensional theories match up, to whatever order in k/Λ we are working, as

$$\psi(0, \mathbf{k}) = \sqrt{\frac{2mT}{\hbar}} \phi(\mathbf{k}). \tag{4.2}$$

This was our definition of ϕ in the more cavalier discussion in the introduction. The frequency k_0 of $\psi(k_0, \mathbf{k})$ denotes

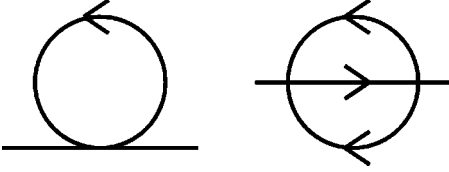


FIG. 3. Fundamental UV-divergent diagrams in the three-dimensional theory (2.5). Dimensional regularization automatically removes the linear divergence of the first diagram and regulates the logarithmic divergence of the second diagram as $1/\epsilon$.

imaginary-time frequency. So one of our matching conditions will be that the inverse Green functions match up as

$$G_{\psi}^{-1}(0, \mathbf{k}) = \frac{G_{\phi}^{-1}(\mathbf{k})}{2m} \quad (4.3)$$

to the relevant order in k/Λ . In the presence of interaction, this definition of ϕ might fix the normalization of the $(\nabla\phi)^*(\nabla\phi)$ term in the action (2.5) to be different from 1. Our three-dimensional effective theory should therefore be written in the somewhat more general form

$$S = \int d^{3-\epsilon}x \left[Z_{\phi}(\nabla\phi)^* \cdot (\nabla\phi) + r_{\text{eff}}\phi^*\phi + \frac{u_{\text{eff}}}{6}(\phi^*\phi)^2 + (\text{higher-dimensional operators}) \right], \quad (4.4)$$

where Z_{ϕ} can deviate from one beyond leading order. In principle, we need to determine the parameters Z_{ϕ} , r_{eff} , and u_{eff} (and any higher-dimensional operators, if they were required at a desired order) by matching.

B. UV regularization

Before starting on matching, we must first unambiguously define the parameters of our theories. The three-dimensional long-distance $O(2)$ theory (2.5) is superrenormalizable, but there are UV divergences associated with the $\phi^*\phi$ interaction. Diagrammatically, these divergencies are associated with the graphs of Fig. 3. In order to give the coefficient r a well-defined meaning, we need to specify a regularization and renormalization scheme. By far the most convenient regularization scheme for perturbative matching calculations is dimensional regularization. We shall replace the number $d=3$ of spatial dimensions by $d=3-\epsilon$, taking $\epsilon \rightarrow 0$ at the end of the day.

To define a finite, renormalized value of r , we will use the modified minimal subtraction ($\overline{\text{MS}}$) scheme with a renormalization scale \bar{M} . The theory is then

$$S = \int d^{3-\epsilon}x \left[Z_{\phi}(\nabla\phi)^* \cdot (\nabla\phi) + r_{\text{bare}}\phi^*\phi + M^{\epsilon} \frac{u_{\text{eff}}}{6}(\phi^*\phi)^2 \right], \quad (4.5)$$

with the relation

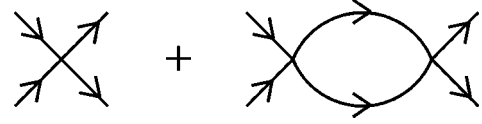


FIG. 4. The two-particle scattering amplitude at second-order in the interaction strength. (Note that there is no t-channel analog of the second diagram, since such a diagram vanishes in a nonrelativistic theory.)

$$r_{\text{bare}} = r_{\overline{\text{MS}}} + \frac{1}{(4\pi)^2 \epsilon} \left(\frac{u}{3}\right)^2 \quad (4.6)$$

between the bare coupling r_{bare} and the renormalized coupling $r_{\overline{\text{MS}}}(\bar{M})$, and where

$$M \equiv \frac{e^{\gamma_E/2}}{\sqrt{4\pi}} \bar{M}. \quad (4.7)$$

[The factor of $e^{\gamma_E/2}/\sqrt{4\pi}$ in Eq. (4.7) is what distinguishes modified minimal subtraction ($\overline{\text{MS}}$) from unmodified minimal subtraction (MS); the difference between the two schemes amounts to nothing more than a multiplicative redefinition of the renormalization scale.]

The original (3+1)-dimensional effective theory (2.2) is not renormalizable and also requires UV regularization, and we will again use dimensional regularization. At second order in the interaction strength (the order relevant to our calculation), the only UV divergence is a well-known linear divergence associated with the second diagram of Fig. 4, which can be absorbed into a redefinition of the coefficient of the $(\psi^*\psi)^2$ interaction. To relate this coefficient to the physical scattering length a , one needs to regularize the theory and then compute the zero-energy limit $\sigma(0)$ of the two-particle cross-section (at zero temperature and density) since a is defined by $8\pi a^2 \equiv \sigma(0)$ for identical particles. In dimensional regularization, however, the loop integral for the second diagram in Fig. 4 vanishes at zero temperature and density, and so there is no second-order correction to $\sigma(0)$. The coefficient of the quartic interaction therefore remains at its tree-level value $2\pi\hbar^2 a/m$, as in Eq. (2.2) [17].

This property of dimensional regularization is a simple consequence of dimensional analysis. At zero energy (i.e., zero external momenta) the second diagram in Fig. 4 is proportional to the loop integral

$$\int \frac{dl_0 d^{3-\epsilon}l}{(il_0 + \omega_l)(-il_0 + \omega_l)}. \quad (4.8)$$

All of the parameter dependence of this integral can be factored out by rescaling l_0 by a factor of $2m$. The rescaled integral

$$\int \frac{dl_0 d^{3-\epsilon}l}{(il_0 + l^2)(-il_0 + l^2)} \quad (4.9)$$

has dimensions of $(\text{length})^{-1+\epsilon}$ but no dimensional parameters to make up that dimension. The only dimensionally consistent answer is zero. In most regularization schemes

other than dimensional regularization, there *are* still dimensional parameters in the integral associated with cutoff scales, and the integral would not be zero. For example, if we regulated with a UV cutoff Λ on l , the integral would give a nonzero result proportional to Λ in $d=3$.

C. Matching of Z_ϕ

We want to calculate the critical value $\bar{\mu}_c$ to next-to-leading order [i.e., $\mu^{(2)}$ in the expansion (3.7)]. One might expect this to require knowing the parameters Z_ϕ , r_{eff} , and u_{eff} of the effective theory to next-to-leading order. In fact, as we shall see, dimensional regularization organizes the calculation in such a way that we only need to compute r_{eff} , which is the three-dimensional analog of μ . But let us briefly discuss the matching of Z_ϕ anyway, as a simple warm up.

The matching of Z_ϕ is trivial because the first-order contribution to the inverse propagator, given by the first diagram of Fig. 3, does not have any momentum dependence. That is, equating the inverse propagators of the two theories as in Eq. (4.3) gives

$$\begin{aligned} \frac{k^2}{2m} + (\mathbf{k} \text{ independent}) + \mathcal{O}(a^2) \\ = \frac{1}{2m} [Z_\phi k^2 + (\mathbf{k} \text{ independent}) + \mathcal{O}(a^2)], \end{aligned} \tag{4.10}$$

where $\mathcal{O}(a^2)$ indicates corrections that are formally second order in perturbation theory. So

$$Z_\phi = 1 + \mathcal{O}(a^2). \tag{4.11}$$

In this paper, we will write $\mathcal{O}(\dots)$ when displaying the full parameter dependence of a correction (except possibly for logarithmic factors) and write $\mathcal{O}(\dots)$ when just showing the dependence on a particular parameter. So $32a^2/\lambda^2 = \mathcal{O}(a^2/\lambda^2) = \mathcal{O}(a^2)$. In matching calculations, where we are formally doing perturbation theory with IR regularization, $\mathcal{O}(a^n)$ will just mean n th order in perturbation theory.

D. Matching of r

To match r , take the $\mathbf{k}=0$ case of matching (4.3) the inverse Green functions:

$$-\mu + \Pi_\psi(0,0) = \frac{1}{2m} [r_{\text{bare}} + \Pi_\phi(0)], \tag{4.12}$$

where Π is the proper self-energy.

We will use dimensional regularization to regulate the infrared divergencies of perturbation theory, as well as the UV divergencies already discussed. A well-known advantage of such use of dimensional regularization for matching calculations is that every loop diagram contributing to $\Pi_\phi(0)$ vanishes by dimensional analysis arguments similar to the one given in Sec. IV B. Consider, for example, the contribution of Fig. 5. In the three-dimensional effective theory, this diagram is proportional to the loop integrals

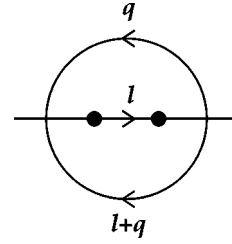


FIG. 5. A two-loop example of a diagram contributing to $-\Pi_\phi(0)$ for a matching calculation. r is treated perturbatively.

$$\int \frac{d^{3-\epsilon} l d^{3-\epsilon} q}{l^6 q^2 |\mathbf{l} + \mathbf{q}|^2}, \tag{4.13}$$

which must vanish because there are no dimensionful parameters to make up the dimensions of the result. It is crucial here that there are no external momenta, that r may be treated as a perturbation for the purpose of matching calculations, and that loop integrals are never dimensionless in dimensional regularization. The upshot is that the matching condition (4.12) becomes simply

$$r_{\text{bare}} = 2m[-\mu + \Pi_\psi(0,0)]. \tag{4.14}$$

Another convenience of the vanishing, in dimensional regularization, of loop diagrams in the three-dimensional theory is that we need not keep track of the matching of u and Z_ϕ if we are only interested in the matching of r . For instance, the one-loop contribution of the first diagram in Fig. 3 gives a contribution proportional to u in three dimensions, and so a second-order calculation of Π_ϕ would require a second-order determination of u , if it were not for the fact that this diagram vanishes.

Returning to the 3+1 dimensional theory, the diagrams, which contribute to Π_ψ up to second order, are shown in Fig. 6, and all diagrams are to be evaluated at finite temperature. Diagram (a) gives the first-order contribution to Π_ψ . It gives

$$\Pi_\psi^{(a)} = \frac{8\pi a}{m} \sum_P \frac{1}{ip_0 + \omega_p}, \tag{4.15}$$

where we introduce the shorthand notations

$$\sum_P \equiv T \sum_{p_0} \int_{\mathbf{p}} \equiv T \sum_{p_0} M^\epsilon \int \frac{d^d p}{(2\pi)^d}, \tag{4.16}$$

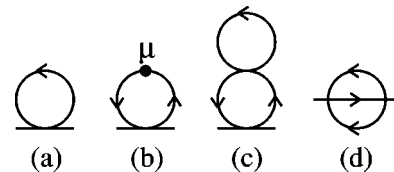


FIG. 6. Diagrams contributing to $-\Pi_\psi$. μ has been treated perturbatively.

$$0 = \chi^{-1} = \bar{\mu} + \text{diagram} + \mathcal{O}(a^2)$$

FIG. 7. The vanishing of the inverse susceptibility at the phase transition, expressed in terms of diagrams at first order in a . (Unlike Fig. 14, these diagrams are evaluated at the center of the trap and not integrated over \mathbf{x} .)

where $d=3-\epsilon$ is the number of spatial dimensions. The p_0 sum can be performed by standard contour tricks,⁵ yielding

$$\Pi_{\psi}^{(a)} = \frac{8\pi a}{m} \int_{\mathbf{p}} [n(\omega_{\mathbf{p}}) + \frac{1}{2}], \quad (4.17)$$

where $n(\omega)$ is the Bose distribution function

$$n(\omega) \equiv \frac{1}{e^{\beta\omega} - 1}. \quad (4.18)$$

The integral of a constant vanishes in dimensional regularization (again by dimensional analysis) and the integral of $n(\omega_{\mathbf{p}})$ can be carried out in three dimensions to yield

$$\Pi_{\psi}^{(a)} = \frac{4aT}{\lambda} \zeta\left(\frac{3}{2}\right) + \mathcal{O}(\epsilon). \quad (4.19)$$

At the critical point, diagrams (b) and (c) cancel each other and so need not be computed individually. The cancellation arises because the inverse susceptibility $\chi_{\psi}^{-1} = -\mu + \Pi_{\psi}(0,0)$ will vanish at a second-order phase transition. This condition is shown diagrammatically in Fig. 7 at first order in perturbation theory. As we have discussed in Sec.

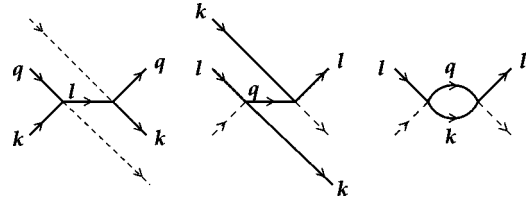


FIG. 8. Time-ordered perturbation theory diagrams corresponding to the three terms of Eq. (4.22). Time flows from left to right, and the dashed line represents the zero external momentum (and zero frequency) in diagram (d) of Fig. 6 for $-\Pi_{\psi}(0,0)$. Each incoming momentum (other than the zero one) is associated with a Bose distribution factor n .

II C, perturbation theory breaks down in the calculation of μ at second order, but the first-order relation of Fig. 7 is, therefore, reliable.⁶ This relation implies that diagrams (b) and (c) of Fig. 6 cancel at second order:

$$\Pi_{\psi}^{(b)} + \Pi_{\psi}^{(c)} = \mathcal{O}(a^3) \quad \text{at} \quad \mu = \bar{\mu}_c. \quad (4.20)$$

The sunset diagram. We now turn to diagram (d) in Fig. 6, the sunset diagram:

$$\begin{aligned} \Pi_{\psi}^{(d)}(0) = & -\frac{1}{2} \left(\frac{8\pi a}{m} \right)^2 \sum_{\mathbf{Q}} \sum_{\mathbf{K}} \\ & \times \frac{1}{(i\mathbf{q}_0 + \omega_q)(i\mathbf{k}_0 + \omega_k)[i(\mathbf{q}_0 + \mathbf{k}_0) + \omega_{\mathbf{q}+\mathbf{k}}]}. \end{aligned} \quad (4.21)$$

We review in Appendix D how the loop frequency sums can be done with standard contour tricks, with the result

$$\Pi_{\psi}^{(d)}(0) = -\frac{1}{2} \left(\frac{8\pi a}{m} \right)^2 \int_{\mathbf{qkl}} \text{P} \frac{[n(\omega_q)n(\omega_k) - 2n(\omega_k)n(\omega_l) - n(\omega_l)]}{\omega_l - \omega_q - \omega_k} (2\pi)^d \delta^{(d)}(\mathbf{l} - \mathbf{q} - \mathbf{k}). \quad (4.22)$$

The symbol P indicates the principal-value prescription

$$\text{P} \frac{1}{x} = \text{Re} \frac{1}{x + i0^{\pm}}, \quad (4.23)$$

where 0^{\pm} is an infinitesimal. This prescription removes the spurious divergence associated with $\omega_l - \omega_q - \omega_k \rightarrow 0$ (but not also $l \sim q \sim k \rightarrow 0$), which is an artifact of this form of writing $\Pi^{(d)}(0)$. (See Appendix D.) We will not bother to explicitly write the principle value in what follows. We note, as a side remark, that, in the language of time-ordered per-

turbation theory (in real time) the three terms of Eq. (4.22) correspond to the three diagrams of Fig. 8.

It is easy to see that the first term of Eq. (4.22) vanishes,

⁶You may wonder why we have discussed the reliability of perturbation theory here when we have already asserted that perturbation theory is valid for the matching calculation. The reason is that we are jumping ahead a little in order to streamline the calculation. The matching calculation can be done perturbatively because it involves only physics at the perturbative scale λ , but the subsequent solution for r_c (and therefore $\bar{\mu}_c$) cannot, since it involves physics at the nonperturbative scale $1/u$. Since we are using a result about $\bar{\mu}_c$ to simplify our matching calculation at $\bar{\mu}_c$, we need to be careful.

⁵For example, see Sec. 25 of Ref. [26].

because it is proportional to

$$\begin{aligned} \int_{\mathbf{qk}} \frac{n(\omega_q)n(\omega_k)}{\omega_{\mathbf{q+k}} - \omega_q - \omega_k} &\propto \int_{\mathbf{qk}} \frac{n(\omega_q)n(\omega_k)}{|\mathbf{q+k}|^2 - q^2 - k^2} \\ &= \int_{\mathbf{qk}} \frac{n(\omega_q)n(\omega_k)}{2\mathbf{q}\cdot\mathbf{k}}, \end{aligned} \quad (4.24)$$

which vanishes by $\mathbf{q} \rightarrow -\mathbf{q}$ (for any reasonable choice of regularization scheme). In Appendix D, we show that the last term of Eq. (4.22) vanishes as $\epsilon \rightarrow 0$ in dimensional regularization. Only the second term of Eq. (4.22) remains, giving

$$\Pi_{\psi}^{(d)}(0) = \left(\frac{8\pi a}{m}\right)^2 \int_{\mathbf{kl}} \frac{n(\omega_k)n(\omega_l)}{\omega_l - \omega_{\mathbf{k-1}} - \omega_k} + \mathcal{O}(\epsilon). \quad (4.25)$$

Subtracting divergences of the sunset diagram. Because $n(\omega_p) \rightarrow (\beta\omega_p)^{-1} \propto p^{-2}$ as $p \rightarrow 0$, the above integral (4.25) has a logarithmic infrared divergence associated with $k \sim l \rightarrow 0$. Unfortunately, the full integral in Eq. (4.25) is too complicated for us to do in arbitrary dimensions, which would be the most straightforward way to apply our chosen regularization scheme, dimensional regularization. It is convenient to instead explicitly isolate the divergent IR behavior by rewriting

$$\begin{aligned} \Pi_{\psi}^{(d)}(0) &= \left(\frac{8\pi a}{m}\right)^2 \left[\int_{\mathbf{kl}} \frac{n(\omega_k)n(\omega_l) - n_0(\omega_k)n_0(\omega_l)}{\omega_l - \omega_{\mathbf{k-1}} - \omega_k} \right. \\ &\quad \left. + \int_{\mathbf{kl}} \frac{n_0(\omega_k)n_0(\omega_l)}{\omega_l - \omega_{\mathbf{k-1}} - \omega_k} + \mathcal{O}(\epsilon) \right], \end{aligned} \quad (4.26)$$

where

$$n_0(\omega) \equiv \frac{1}{\beta\omega}. \quad (4.27)$$

The second integral vanishes in dimensional regularization for the usual reason: it is proportional to

$$\int_{\mathbf{kl}} \frac{1}{k^2 l^2 (l^2 - |\mathbf{k-1}|^2 - k^2)}, \quad (4.28)$$

which contains no dimensionful parameter to make up its dimensions. So

$$\Pi_{\psi}^{(d)}(0) = \left(\frac{8\pi a}{m}\right)^2 \int_{\mathbf{kl}} \frac{n(\omega_k)n(\omega_l) - n_0(\omega_k)n_0(\omega_l)}{\omega_l - \omega_{\mathbf{k-1}} - \omega_k} + \mathcal{O}(\epsilon). \quad (4.29)$$

The above integral is infrared convergent and, if it were not for the fact that we have now introduced a UV divergence associated with $k \sim l \rightarrow \infty$, we would be able to set $d=3$ in that integral and ignore regularization issues.

To continue, it is useful to understand another way to interpret the infrared behavior represented by the last term of Eq. (4.26):

$$I_0 = \left(\frac{8\pi a}{m}\right)^2 \int_{\mathbf{kl}} \frac{n_0(\omega_k)n_0(\omega_l)}{\omega_l - \omega_{\mathbf{k-1}} - \omega_k}. \quad (4.30)$$

As discussed before, infrared physics is dominated, in imaginary time, by the zero-frequency mode of the field ψ . I_0 turns out to be the $q_0 = k_0 = 0$ piece of the original frequency sums (4.21) representing diagram (d). A quick way to see this is to note that the integrand in I_0 above is the high-temperature limit ($\beta \rightarrow 0$) of the original integrand in Eq. (4.25). But, if one goes all the way back to the original imaginary-time frequency sums (4.21), the integrand there is proportional to

$$\sum_{q_0} \sum_{k_0} \frac{1}{(iq_0 + \omega_q)(ik_0 + \omega_k)[i(q_0 + k_0) + \omega_{\mathbf{q+k}}]}, \quad (4.31)$$

with q_0 and k_0 of the form $2\pi nT$. Only the $q_0 = k_0 = 0$ piece survives in the $\beta \rightarrow 0$ limit of this integrand, and this establishes the correspondence.

It is important to note that nonzero frequency modes *do* contribute to diagram (d) even in the infinitely high-temperature limit, because the limit does not commute with the integration over spatial momenta \mathbf{q} and \mathbf{k} . However, in our analysis so far, we have not yet performed the \mathbf{q} and \mathbf{k} integrations, and it is okay to take limits of integrands to see the correspondence of I_0 with the $q_0 = k_0 = 0$ piece of diagram (d).

The upshot is that the infrared piece I_0 that we isolated from diagram (d) is proportional to the same diagram evaluated in a purely three-dimensional theory:

$$\begin{aligned} I_0 &= -\frac{T^2}{2} \left(\frac{8\pi a}{m}\right)^2 \int_{\mathbf{qk}} \frac{1}{\omega_q \omega_k \omega_{\mathbf{q+k}}} \\ &= -4m^3 T^2 \left(\frac{8\pi a}{m}\right)^2 \int_{\mathbf{qk}} \frac{1}{q^2 k^2 |\mathbf{q+k}|^2}. \end{aligned} \quad (4.32)$$

This diagram is logarithmically divergent in both the infrared and ultraviolet, just as the original expression (4.30) for I_0 , and it vanishes in dimensional regularization. The UV divergence of our current expression (4.29) for diagram (d) came from the UV divergence of I_0 . To isolate this UV divergence, we'd like to isolate a term that (i) has the same UV divergence as I_0 , (ii) is analytically computable in dimensional regularization, and (iii) is infrared convergent (since otherwise we'll just reintroduce an infrared divergence when we isolate it). Something that satisfies all these requirements is the same integral (4.32) of a three-dimensional theory as above, but with mass terms to cut off the infrared:

$$I_{\mathcal{N}} \equiv -\frac{T^2}{2} \left(\frac{8\pi a}{m} \right)^2 \int_{\mathbf{qk}} \frac{1}{(\omega_q + \mathcal{N})(\omega_k + \mathcal{N})(\omega_{\mathbf{q+k}} + \mathcal{N})} = -4m^3 T^2 \left(\frac{8\pi a}{m} \right)^2 \int_{\mathbf{qk}} \frac{1}{(q^2 + \mathcal{M}^2)(k^2 + \mathcal{M}^2)(|\mathbf{q+k}|^2 + \mathcal{M}^2)}, \quad (4.33)$$

where $\mathcal{N} = \mathcal{M}^2/2m$ is an arbitrary frequency scale. Our strategy will then be to rewrite our current expression (4.29) as

$$\Pi_{\psi}^{(d)}(0) = \left[\left(\frac{8\pi a}{m} \right)^2 \int_{\mathbf{kl}} \frac{n(\omega_k) n(\omega_l) - n_0(\omega_k) n_0(\omega_l)}{\omega_l - \omega_{\mathbf{k-1}} - \omega_k} + I_{\mathcal{N}} \right] - I_{\mathcal{N}} + \mathcal{O}(\epsilon). \quad (4.34)$$

To put the first $I_{\mathcal{N}}$ term in a form similar to the integral shown explicitly in Eq. (4.34), one may replace ω by $\omega + \mathcal{N}$ in our early discussion of $\Pi_{\psi}^{(d)}(0)$ and take the $\beta \rightarrow 0$ limit in all integrands to get the following analogy to Eq. (4.22):

$$I_{\mathcal{N}} = -\frac{1}{2} \left(\frac{8\pi a}{m} \right)^2 \int_{\mathbf{qkl}} \frac{[n_0(\omega_q + \mathcal{N}) n_0(\omega_k + \mathcal{N}) - 2n_0(\omega_k + \mathcal{N}) n_0(\omega_l + \mathcal{N})]}{(\omega_l + \mathcal{N}) - (\omega_q + \mathcal{N}) - (\omega_k + \mathcal{N})} (2\pi)^d \delta^{(d)}(\mathbf{1} - \mathbf{q} - \mathbf{k}) + \mathcal{O}(\epsilon). \quad (4.35)$$

We then obtain

$$\begin{aligned} \Pi_{\psi}^{(d)}(0) = & \left(\frac{8\pi a}{m} \right)^2 \left\{ \int_{\mathbf{kl}} \left[\frac{n(\omega_k) n(\omega_l) - n_0(\omega_k) n_0(\omega_l)}{\omega_l - \omega_{\mathbf{k-1}} - \omega_k} \right. \right. \\ & \left. \left. + \frac{n_0(\omega_k + \mathcal{N}) n_0(\omega_l + \mathcal{N})}{\omega_l - \omega_{\mathbf{k-1}} - \omega_k - \mathcal{N}} \right] \right. \\ & \left. - \frac{1}{2} \int_{\mathbf{kl}} \frac{n_0(\omega_{\mathbf{k-1}} + \mathcal{N}) n_0(\omega_k + \mathcal{N})}{\omega_l - \omega_{\mathbf{k-1}} - \omega_k - \mathcal{N}} \right\} - I_{\mathcal{N}} + \mathcal{O}(\epsilon). \end{aligned} \quad (4.36)$$

The first integral (with its implicit principal-value prescription) is now both infrared and ultraviolet convergent and can now be evaluated in exactly $d=3$ dimensions. The second integral is convergent as well. So fix $d=3$ in these integrals, scale out the parameters, and do the angular integrations using the principal-value prescription. This puts the integrals in a form appropriate for straightforward numerical evaluation. The result for the dimensionally regulated integral (4.33) for $I_{\mathcal{N}}$ is

$$\begin{aligned} & \int_{\mathbf{qk}} \frac{1}{(q^2 + \mathcal{M}^2)(k^2 + \mathcal{M}^2)(|\mathbf{q+k}|^2 + \mathcal{M}^2)} \\ & = \frac{1}{(4\pi)^2} \left[\frac{1}{2\epsilon} + \ln \frac{\bar{M}}{3\mathcal{M}} + \frac{1}{2} \right] + \mathcal{O}(\epsilon), \end{aligned} \quad (4.37)$$

which can be extracted from the general d result of Ref. [27] or the $\epsilon \rightarrow 0$ analysis in Ref. [28]. Putting everything together,

$$\Pi_{\psi}^{(d)}(0) = \frac{32\pi a^2 T}{\lambda^2} \left[\frac{1}{2\epsilon} + \ln(\bar{M}\lambda) + C_1 \right], \quad (4.38)$$

where C_1 is the numerical constant

$$\begin{aligned} C_1 = & \frac{1 - \ln(36\pi\bar{N})}{2} \\ & + \frac{2}{\pi^2} \int_0^\infty dk dl \left[\left(\frac{kl}{(e^{k^2} - 1)(e^{l^2} - 1)} - \frac{1}{kl} \right) \ln \left| \frac{k-l}{k+l} \right| \right. \\ & \left. + \frac{kl}{(k^2 + \bar{N})(l^2 + \bar{N})} \ln \left| \frac{\bar{N} + 2k(k-l)}{\bar{N} + 2k(k+l)} \right| \right] \\ & + \frac{1}{\pi^2} \int_0^\infty dq dk \frac{qk}{(q^2 + \bar{N})(k^2 + \bar{N})} \ln \left| \frac{\bar{N} + 2qk}{\bar{N} - 2qk} \right|, \end{aligned} \quad (4.39a)$$

which is independent of the choice of the dimensionless number $\bar{N} \equiv \beta\mathcal{N}$. Numerical evaluation of the integrals gives

$$C_1 \simeq -0.54410. \quad (4.39b)$$

(Since completion of this work, a somewhat more compact formula for C_1 has been derived in Ref. [4].)

We should mention that it is possible, at a formal level, to turn the original unregulated integral of Eq. (4.25) into a double sum, similar to the sums appearing in the earlier formula (3.4) for the density, by using methods similar to those reviewed in Appendix A. However, the infrared divergence of $\Pi_{\psi}^{(d)}(0)$ would manifest as $i, j \rightarrow \infty$ divergencies of these sums. We found it easier to handle the infrared issues in the integral form than in the summation form. This is the only reason why our treatment of $\Pi_{\psi}(0)$ superficially looks so dissimilar, in final form, to our treatment of pressure and density in Sec. III.

1. Final result for r

Combining our results for the pieces of $\Pi_{\psi}(0)$ with the matching formula (4.14) for r , we obtain

$$\begin{aligned} r_{\text{bare}} = & -2m\mu + 2mT \left\{ \frac{4a}{\lambda} \zeta\left(\frac{3}{2}\right) + \frac{32\pi a^2}{\lambda^2} \left[\frac{1}{2\epsilon} + \ln(\bar{M}\lambda) \right. \right. \\ & \left. \left. + C_1 \right] \right\} + \mathcal{O}(a^3) + \mathcal{O}(\mu - \bar{\mu}_c). \end{aligned} \quad (4.40)$$

Comparing this to the expression (4.6) for the $\overline{\text{MS}}$ definition of r , and using the leading-order result (2.6) for u ,

$$r_{\overline{\text{MS}}}(\overline{M}) = -2m\mu + 2mT \left\{ \frac{4a}{\lambda} \zeta\left(\frac{3}{2}\right) + \frac{32\pi a^2}{\lambda^2} [\ln(\overline{M}\lambda) + C_1] \right\} + \mathcal{O}(a^3) + \mathcal{O}(\mu - \overline{\mu}_c). \quad (4.41)$$

E. Final result for $\overline{\mu}_c$

We can now solve Eq. (4.41) for the coefficients in the expansion

$$\overline{\mu}_c = \left[\overline{\mu}_c^{(1)} \frac{a}{\lambda} + \overline{\mu}_c^{(2)} \left(\frac{a}{\lambda} \right)^2 + \dots \right] k_B T \quad (4.42a)$$

of $\overline{\mu}_c$. The first-order result, well known in the literature, is

$$\overline{\mu}_c^{(1)} = 4\zeta\left(\frac{3}{2}\right), \quad (4.42b)$$

and is a simple consequence of the vanishing susceptibility as depicted in Fig. 7. The second-order coefficient is

$$\overline{\mu}_c^{(2)} = 32\pi \left[\ln(\overline{M}\lambda) + C_1 - 72\pi^2 \frac{r_{c,\overline{\text{MS}}}(\overline{M}, u)}{u^2} \right], \quad (4.42c)$$

where $r_{c,\overline{\text{MS}}}(\overline{M}, u)$ is the critical value of $r_{\overline{\text{MS}}}$ for a given choice of coupling u and renormalization scale \overline{M} . The only dimensionful scale of the three-dimensional theory at its critical point is u , and so one should pick the renormalization scale \overline{M} of order u . Note that the critical value $r_{c,\overline{\text{MS}}}$ is then proportional to u^2 by dimensional analysis. Taking $\overline{M} = u/3$ for definiteness, and because that was the choice made in presenting lattice simulation results in Ref. [7], we have

$$\overline{\mu}_c^{(2)} = 32\pi \left[\ln\left(\frac{32\pi^2 a}{\lambda}\right) + C_1 - 72\pi^2 \mathcal{R} \right], \quad (4.43)$$

where the dimensionless constant

$$\mathcal{R} \equiv \frac{r_{c,\overline{\text{MS}}}(\overline{M} = u/3, u)}{u^2} \quad (4.44a)$$

is nonperturbative and must be extracted from simulations of the three-dimensional effective theory (2.5). The simulation result is, from Eq. (1.5) of Ref. [7],

$$\mathcal{R} = 0.001920(2). \quad (4.44b)$$

V. FINAL RESULT FOR T_c

We can now combine the second-order result (4.43) for $\overline{\mu}_c$ with our earlier expression (3.11) for T_c to obtain

$$T_c = T_0 \left[1 + c_1 \frac{a}{\lambda_0} + \left(c_2' \ln \frac{a}{\lambda_0} + c_2'' \right) \left(\frac{a}{\lambda_0} \right)^2 + \mathcal{O}\left(\frac{a}{\lambda_0} \right)^3 \right], \quad (5.1a)$$

with

$$c_1 \approx -3.426\,032, \quad (5.1b)$$

$$c_2' = -\frac{32\pi\zeta(2)}{3\zeta(3)}, \quad (5.1c)$$

$$c_2'' = C_2 - \frac{32\pi\zeta(2)}{3\zeta(3)} [\ln(32\pi^2) + C_1 - 72\pi^2 \mathcal{R}] \approx -155.0, \quad (5.1d)$$

and with T_0 , λ_0 the ideal-gas quantities given at the end of Sec. III. The constants c_1 , C_2 , C_1 , and \mathcal{R} are given by Eqs. (3.11b), (3.12), (4.39), and (4.44), respectively. All have been computed perturbatively, except for \mathcal{R} , which is the nonperturbative information extracted from lattice simulations.

VI. YET HIGHER-ORDER CORRECTIONS

We have based our discussion on the (3+1)-dimensional theory (2.2) of ψ and the effective 3-dimensional theory (2.5) of the zero-frequency Matsubara modes. Both of these theories are approximate and have corrections that we have ignored, claiming them to be higher order than the order of interest. In this section, we will briefly discuss the nature of those corrections.

Let us begin with the original (3+1)-dimensional theory (2.2) of ψ . Among other things, this theory ignores (a) the energy dependence of the low-energy atomic scattering cross section, and (b) the effects of three-body collisions. Braaten *et al.* [29], give a nice discussion of how to systematize the corrections to the low-energy (3+1)-dimensional theory, discussing interactions that are progressively more and more irrelevant at low energies. The most important of such corrections are to supplement the Lagrangian (2.2) by the additional interactions

$$\delta\mathcal{L} = -\frac{\pi\hbar^2 a^2 r_s}{2m} |\nabla(\psi^* \psi)|^2 - B(\psi^* \psi)^3. \quad (6.1)$$

B parametrizes the amplitude for three-body collisions. r_s is the effective range of the two-body scattering problem and parametrizes the linear term in the energy dependence of the cross section at low energy. The importance of the r_s term grows with energy, which turns out to mean that its leading effect on the critical temperature or the chemical potential is not infrared dominated and can be treated perturbatively.

The parametric size of the leading-order effects of these corrections can be estimated in a very simple way by comparing them to the usual quartic term $(\psi^* \psi)^2$. At leading order, the effects of $(\psi^* \psi)^2$ on the quantities computed in this paper [μ_c for a homogeneous gas and $N(T_c)$ for a trapped gas] were dominated by momentum scales of order $\bar{k} \sim 1/\lambda$ (as opposed to the infrared scale u). Relative to the $a(\psi^* \psi)^2$ interaction, one would expect that the leading-order effects of the $a^2 r_s |\nabla(\psi^* \psi)|^2$ interaction of Eq. (6.1) should therefore be suppressed by $ar_s \bar{k}^2 \sim ar_s/\lambda^2$. Near the transition, this is down by two powers of the typical interparticle separation $l \sim \bar{n}^{-1/3} \sim N^{-1/6} a_{\text{ho}}$ discussed in the introduction (since $\lambda \sim l$ at T_c), whereas the second-order effects

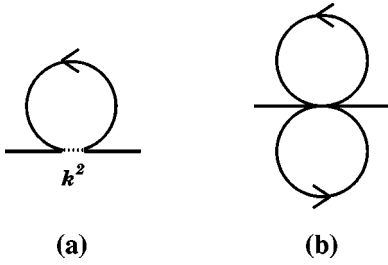


FIG. 9. Leading-order corrections to the $\Pi_{\psi}(0)$ (and hence the determination of $\bar{\mu}_c$) due to (a) the effective range and (b) the three-body scattering terms of Eq. (6.1). The dotted line represents the momentum flow k in the $|\nabla(\phi^*\psi)|^2$ vertex.

computed in this paper are down only by one power, compared to the leading-order effect of interactions. Again relative to the $(\psi^*\psi)^2$ interaction, one would expect that the three-body $(\psi^*\psi)^3$ interaction of Eq. (6.1) is down by a factor of $(Bm/\hbar^2 a)\psi^*\psi \sim (Bm/\hbar^2 a)n$, which is down by three powers of l since $n \sim l^{-3}$. The moral is that corrections to the original 3+1 dimensional Lagrangian (2.2) do not matter for a second-order calculation of T_c for a dilute trapped gas, that the result at third order would depend on the effective range r_s and not just the scattering length a , and that the result at fourth order would depend on the three-body scattering rate as well.

One can also verify the above analysis by a consideration of the leading-order diagrams involving a given correction from Eq. (6.1). Figure 9 shows diagrams contributing to $\bar{\mu}_c$ and Fig. 10 those⁷ contributing to $n(T, \mu)$. As an example, the diagram of Fig. 9(a) gives a contribution to the chemical potential proportional to

$$\delta\mu \sim \frac{a^2 r_s}{\hbar m} \int \frac{k^2}{ik_0 + \omega_l}. \quad (6.2)$$

The diagram is not dominated by infrared momenta, and so the perturbative treatment is justified. The dominant wave numbers are $\bar{k} \sim 1/\lambda$, as claimed above, corresponding to energies $k_B T$ and frequencies $\omega_{\bar{k}} \sim k_B T/\hbar$. The result is that

$$\delta\mu \sim \frac{a^2 r_s}{\hbar m} \frac{k_B T \bar{k}^5}{\omega_{\bar{k}}} \sim \frac{a^2 r_s}{\lambda^3} k_B T, \quad (6.3)$$

where the \bar{k}^5 comes from the $k^2 d^3k$ in the integral. Compared to the leading-order result $O(k_B T a/\lambda)$ for the chemical potential, Eq. (6.3) is down by $O(ar_s/\lambda^2)$, just as we argued more simply above.

Finally, even ignoring corrections to the original (3+1)-dimensional theory, there will still be corrections to the ef-

⁷The effect of r_s represented by Fig. 10(a) has been considered historically in discussions of ΔT_c for a homogeneous Bose gas [30]. Those discussions completely missed the dominant contributions to ΔT_c . They also did not use the more general language of effective ranges but implicitly used the Born approximation to express r_s in terms of the two-body potential.

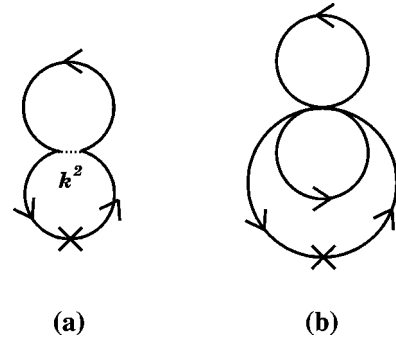


FIG. 10. As in Fig. 9 but showing corrections to the density $n(T, \mu)$.

fective 3-dimensional theory (2.5) of the zero modes. One might worry in particular about a $(\phi^*\phi)^3$ interaction between the zero modes, which is a marginal interaction in three dimensions. Such an effective interaction can be induced by diagrams such as Fig. 11 in the (3+1)-dimensional theory, where the external lines are zero modes and the internal lines are nonzero modes. However, the nonzero modes are infrared insensitive and are dominated by frequencies of the order of $k_B T/\hbar$ and momenta of the order of $\bar{k} \sim 1/\lambda$. Power counting Fig. 11 then gives an interaction in the effective 3-dimensional theory of order

$$\delta\mathcal{L}_{\phi} \sim u^3 \lambda^3 (\phi^*\phi)^3, \quad (6.4)$$

where the u^3 can be understood as arising from the 3 vertices in Fig. 11 and the λ^3 from dimensional analysis based on the dominant momentum scale.

Now consider the effect of the vertex (6.4) on the infrared physics at momentum scales $p \sim 1/u$, to which the 3-dimensional effective theory is intended to be applied. At that scale, the $(\phi^*\phi)^2$ interaction can no longer be treated perturbatively and, by dimensional analysis, the fluctuations in ϕ are of the order of $u^{1/2}$. The relative importance of the $(\phi^*\phi)^3$ term at the infrared scale $p \sim 1/u$ is then

$$\frac{u^3 \lambda^3 (\phi^*\phi)^3}{u (\phi^*\phi)^2} \sim u^3 \lambda^3 \sim \frac{a^3}{\lambda^3}. \quad (6.5)$$

The contributions of the effective $(\phi^*\phi)^3$ operator is therefore down by three powers of $l^{-1} \sim \lambda^{-1}$ compared to those contributions we have included in this paper. Other corrections to the three-dimensional theory are similarly suppressed.

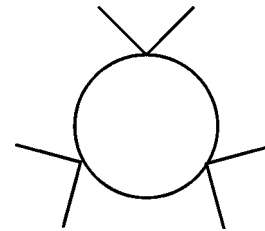


FIG. 11. An effective $(\phi^*\phi)^3$ interaction of zero modes generated by a loop of nonzero modes.

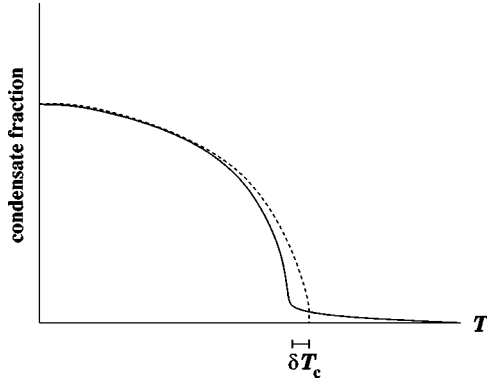


FIG. 12. A schematic depiction of finite-size effects on the BEC phase transition in the ideal-gas limit. The dashed curve indicates the infinite-volume transition.

VII. HOW WIDE IS A WIDE TRAP?

We have assumed throughout this paper that the trap is arbitrarily wide ($\omega_x, \omega_y, \omega_z \rightarrow 0$ with $N\omega_x\omega_y\omega_z$ fixed). We will now take a moment to explain parametrically how wide “wide enough” is for our second-order results to be valid. Our second-order result for $\bar{\mu}_c$ depends on nonperturbative physics near the center of the trap, and we treated the trap as flat over the wavelength $1/u$ of such physics. The trap must, therefore, be wide enough that this wavelength fits comfortably inside the region of the trapped gas that is nearly critical, whose size we labeled R_{np} in Sec. II D.

First consider the case $\omega_x \sim \omega_y \sim \omega_z$. Using Table I, the condition $1/u \ll R_{np}$ can be translated into $l \ll N^{1/6}a$. Combining this with the basic diluteness assumption $a \ll l$ of our analysis, we then require

$$a \ll l \ll N^{1/6}a. \tag{7.1}$$

This shows only the parametric dependence, and we have made no attempt to estimate numerical factors.

For a very anisotropic trap, the strongest constraint will come from requiring the narrowest direction of the near-critical region to be larger than $1/u$. Let ω_{max} be the largest of $\omega_x, \omega_y,$ and ω_z . Repeating the analysis of Sec. II D then gives the corresponding value of R_{np} in that direction as $\hbar a/m\omega_{max}\lambda^2 \sim N^{1/3}a\omega_{ho}/\omega_{max}$. So the condition is

$$a \ll l \ll N^{1/6}a \sqrt{\frac{\omega_{ho}}{\omega_{max}}}. \tag{7.2}$$

These constraints may be translated into other variables using $l \sim \bar{n}^{-1/2} \sim \lambda \sim N^{-1/6}a_{ho}$.

This condition on the size of the trap can also be summarized as a comparison of the uncertainty in the value of T_c due to finite-size effects versus the resolution with which we have computed T_c in our second-order formula (5.1). Finite-size effects round off the nonanalyticity of the infinite-size transition, as depicted in Fig. 12. A standard result from the literature is that, below the rounded transition, finite-size effects create the appearance of a transition temperature shifted by [1,31]

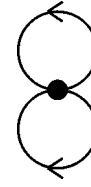


FIG. 13. An additional perturbative diagram contributing to the pressure at second order. The fat black dot represents the one-loop $(\psi^*\psi)^2$ renormalization counterterm, which vanishes in dimensional regularization.

$$\frac{\delta T_c}{T_0} \simeq - \frac{\zeta(2)}{2\zeta(3)^{2/3}} \frac{\bar{\omega}}{\omega_{ho}} N^{-1/3} \tag{7.3}$$

from the infinite-volume value (in the ideal-gas approximation) as depicted in the figure. Here, $\bar{\omega}$ is the arithmetic mean

$$\bar{\omega} \equiv \frac{\omega_x + \omega_y + \omega_z}{3}. \tag{7.4}$$

The condition that this finite-size effect on the transition be small compared to the relative $O(a^2/\lambda_0^2)$ correction to T_0 that we have presented in Eq. (5.1) happens to be the same, parametrically, as the right-hand condition in Eq. (7.2).

VIII. CONCLUSION

The relative size of the second-order effect in our final result (5.1) for T_c obviously depends on the diluteness of the gas and the value of the scattering length, which will vary from experiment to experiment. However, just for fun, let us put numbers to the size of the effect for one specific experimental study of T_c that has appeared in the literature. The 1996 experiment of Ensher *et al.* [32] found $\Delta T_c/T_0 = -0.06 \pm 0.05$ for dilute gases of roughly $N=40,000$ ⁸⁷Rb atoms in the $F=2$ hyperfine state, trapped with $\nu_z = 373$ Hz, $\omega_z = 2\pi\nu_z$, and $\omega_x = \omega_y = \omega_z/\sqrt{8}$. The relevant scattering length is $a = (103 \pm 5)a_0$ [33], where $a_0 = 0.0529177$ nm is the Bohr radius. (See also Ref. [34].) These parameters correspond to $a/\lambda_0 \approx 0.016$. For an arbitrarily wide trap, this would translate into a first-order correction to T_c of roughly -5.4% and a second-order correc-

TABLE III. Feynman rules appropriate for standard perturbation theory in the (3+1)-dimensional theory.

	$\frac{1}{ik_0 + \omega_{\mathbf{k}} - \mu}$
	$-\frac{8\pi a}{m}$

tion of roughly +0.9%. For the actual trap, however, the corrections (7.3) due to finite-size effects are roughly -2.4%. The fact that this is larger in magnitude than the second-order correction, leads us to suspect that this particular trap may not be wide enough for the second-order result to be trusted, as was discussed in Sec. VII.

ACKNOWLEDGMENTS

We thank Eric Braaten, Eric Cornell, Cass Sackett, and Guy Moore for useful discussions. This work was supported, in part, by the U.S. Department of Energy under Grant No. DE-FG02-97ER41027.

APPENDIX A: FIELD THEORY REDERIVATION OF $P(T, \mu)$

The two diagrams that contribute to the pressure at second order in perturbation theory were shown in Figs. 1(b) and 1(c). Technically, there is also a third diagram, Fig. 13, which involves the one-loop $(\psi^* \psi)^2$ counterterm (represented by the fat dot) for renormalizing the linear UV divergence of zero-temperature, zero-density $2 \rightarrow 2$ scattering at second order. However, we shall use dimensional regularization, for which this counter-term vanishes, as discussed in Sec. IV B. The Feynman rules are given in Table III. They are the same as in Table II except that we are not treating the chemical potential μ as a perturbation in this context. We work in units where $\hbar = k_B = 1$.

1. The basketball diagram

Let us start with diagram (c) of Fig. 1. The corresponding contribution to the pressure $P = (\beta V)^{-1} \ln Z$ is⁸

$$P_c = \frac{1}{8} \left(\frac{-8\pi a}{m} \right)^2 \times \sum_{PQKL} \frac{\beta \delta_{p_0+q_0-k_0-l_0} (2\pi)^3 \delta^{(3)}(\mathbf{p}+\mathbf{q}-\mathbf{k}-\mathbf{l})}{(ip_0+\tilde{\omega}_p)(iq_0+\tilde{\omega}_q)(ik_0+\tilde{\omega}_k)(il_0+\tilde{\omega}_l)}, \quad (\text{A1})$$

where we have introduced the shorthand notation

$$P_c = \frac{32\pi^2 a^2}{m^2} \int_{\mathbf{pqkl}} \text{P} \frac{n(\tilde{\omega}_q)n(\tilde{\omega}_k)n(\tilde{\omega}_l) - \frac{1}{2}n(\tilde{\omega}_p)n(\tilde{\omega}_q)}{\tilde{\omega}_p + \tilde{\omega}_q - \tilde{\omega}_k - \tilde{\omega}_l} (2\pi)^3 \delta^{(3)}(\mathbf{p}+\mathbf{q}-\mathbf{k}-\mathbf{l}) \\ = \frac{32\pi^2 a^2}{m^2} \int_{\mathbf{pqkl}} \text{P} \frac{n(\tilde{\omega}_q)n(\tilde{\omega}_k)n(\tilde{\omega}_l) - \frac{1}{2}n(\tilde{\omega}_p)n(\tilde{\omega}_q)}{\omega_p + \omega_q - \omega_k - \omega_l} (2\pi)^3 \delta^{(3)}(\mathbf{p}+\mathbf{q}-\mathbf{k}-\mathbf{l}). \quad (\text{A7})$$

⁸ VP_c corresponds to $Q'/Q^{(0)}$ of Ref. [15]. The contribution VP_b from diagram (b) of Fig. 1 corresponds to $[Q''/Q^{(0)}] - \frac{1}{2}[Q^{(1)}/Q^{(0)}]^2$.

⁹See, for example, Sec. 5.5.1 of Ref. [35].

$$\tilde{\omega}_k \equiv \omega_k - \mu = \frac{k^2}{2m} - \mu, \quad (\text{A2})$$

and where the summation-integration sign is defined in Eq. (4.16). We now use standard tricks to evaluate the frequency sums.⁹ Specifically, rewrite the frequency Kronecker δ as an integral of exponentials, and factorize the expression into independent sums:

$$P_c = \frac{8\pi^2 a^2}{m^2} \int_0^\beta d\alpha \sum_P \frac{e^{-i\alpha p_0}}{ip_0 + \tilde{\omega}_p} \sum_Q \frac{e^{-i\alpha q_0}}{iq_0 + \tilde{\omega}_q} \\ \times \sum_K \frac{e^{+i\alpha k_0}}{ik_0 + \tilde{\omega}_k} \sum_L \frac{e^{+i\alpha l_0}}{il_0 + \tilde{\omega}_l} (2\pi)^3 \delta^{(3)}(\mathbf{p}+\mathbf{q}-\mathbf{k}-\mathbf{l}). \quad (\text{A3})$$

Then we use the standard frequency sums

$$T \sum_{p_0} \frac{e^{-i\alpha p_0}}{ip_0 + \omega} = n(\omega) e^{\alpha\omega}, \quad (\text{A4a})$$

$$T \sum_{p_0} \frac{e^{+i\alpha p_0}}{ip_0 + \omega} = n(\omega) e^{(\beta-\alpha)\omega}, \quad (\text{A4b})$$

for $0 < \alpha < \beta$. The α integration is then trivial, yielding

$$P_c = \frac{8\pi^2 a^2}{m^2} \int_{\mathbf{pqkl}} n(\tilde{\omega}_p)n(\tilde{\omega}_q)n(\tilde{\omega}_k)n(\tilde{\omega}_l) \\ \times \frac{e^{\beta(\tilde{\omega}_p+\tilde{\omega}_q)} - e^{\beta(\tilde{\omega}_k+\tilde{\omega}_l)}}{\tilde{\omega}_p + \tilde{\omega}_q - \tilde{\omega}_k - \tilde{\omega}_l} (2\pi)^3 \delta^{(3)}(\mathbf{p}+\mathbf{q}-\mathbf{k}-\mathbf{l}). \quad (\text{A5})$$

Note that the zero of the denominator at $\tilde{\omega}_p + \tilde{\omega}_q = \tilde{\omega}_k + \tilde{\omega}_l$ is canceled by a corresponding zero of the numerator. However, it will be useful to split the integral into pieces that individually lack this cancellation, and so it is useful to first introduce a redundant principal part (P) prescription in Eq. (A5). Making use of the identity

$$n(\omega) e^{\beta\omega} = n(\omega) + 1, \quad (\text{A6})$$

expanding terms, and permuting integration variables, we can rewrite Eq. (A5) as

The term

$$P_{c,2} = \frac{32\pi^2 a^2}{m^2} \int_{\mathbf{p}\mathbf{q}\mathbf{k}\mathbf{l}} \mathbf{P} \frac{-\frac{1}{2}n(\tilde{\omega}_p)n(\tilde{\omega}_q)}{\omega_p + \omega_q - \omega_k - \omega_l} (2\pi)^3 \times \delta^{(3)}(\mathbf{p} + \mathbf{q} - \mathbf{k} - \mathbf{l}), \quad (\text{A8})$$

involving just two n 's, has a linear UV divergence associated with $k, l \rightarrow \infty$, with p and q fixed. This is the divergence that is canceled by the counterterm diagram of Fig. 13 for generic regularization schemes and that dimensional regularization will simply ignore. In fact, the entire term $P_{c,2}$ simply vanishes in dimensional regularization, which can be seen by doing the \mathbf{k} and \mathbf{l} integrations explicitly in d spatial dimensions. Defining $\mathbf{s} = \mathbf{k} - \frac{1}{2}(\mathbf{p} + \mathbf{q})$,

$$\int_{\mathbf{k}\mathbf{l}} \mathbf{P} \frac{(2\pi)^d \delta^{(d)}(\mathbf{p} + \mathbf{q} - \mathbf{k} - \mathbf{l})}{\omega_p + \omega_q - \omega_k - \omega_l} = -m \int \frac{d^d s}{(2\pi)^d} \mathbf{P} \frac{1}{s^2 - \frac{1}{4}|\mathbf{p} - \mathbf{q}|^2}. \quad (\text{A9})$$

It's convenient to re-express the principal part in terms of infinitesimals, using Eq. (4.23), before doing the \mathbf{s} integration. The integral (A9) then yields

$$\begin{aligned} & -\frac{m\Gamma\left(1 - \frac{d}{2}\right)}{(4\pi)^{d/2}} \text{Re}\left[-\frac{1}{4}|\mathbf{p} - \mathbf{q}|^2 + i0^\pm\right]^{(d-2)/2} \\ & = -\frac{m\Gamma\left(1 - \frac{d}{2}\right)}{(4\pi)^{d/2}} \left[\frac{1}{4}|\mathbf{p} - \mathbf{q}|^2\right]^{(d-2)/2} \cos\left(\frac{(d-2)\pi}{2}\right). \end{aligned} \quad (\text{A10})$$

Analytic continuation to $d=3$ yields zero:

$$\int_{\mathbf{k}\mathbf{l}} \mathbf{P} \frac{(2\pi)^d \delta^{(d)}(\mathbf{p} + \mathbf{q} - \mathbf{k} - \mathbf{l})}{\omega_p + \omega_q - \omega_k - \omega_l} = \mathcal{O}(\epsilon), \quad (\text{A11})$$

where $\epsilon = 3 - d$. To conclude that the contribution (A8) to the pressure vanishes in dimensional regularization, one must also check that the final \mathbf{p} and \mathbf{q} integrals with the $\mathcal{O}(\epsilon)$ integrand do not diverge, since divergencies could possibly generate a $1/\epsilon$ singularity to cancel the $\mathcal{O}(\epsilon)$ behavior of the integrand. However, the UV is cut off by the distribution functions $n(\omega_p)$ and $n(\omega_q)$ in Eq. (A8), and so this is not an issue.

We are left with only the term of Eq. (A7) with three n 's:

$$P_c = \frac{32\pi^2 a^2}{m^2} \int_{\mathbf{p}\mathbf{q}\mathbf{k}\mathbf{l}} \mathbf{P} \frac{n(\tilde{\omega}_q)n(\tilde{\omega}_k)n(\tilde{\omega}_l)}{\omega_p + \omega_q - \omega_k - \omega_l} \times (2\pi)^3 \delta^{(3)}(\mathbf{p} + \mathbf{q} - \mathbf{k} - \mathbf{l}). \quad (\text{A12})$$

This reproduces Eq. (A15) of Huang *et al.* [15]. Since their subsequent discussion of evaluating this integral is somewhat

telegraphic, we will present our own method. First, expand the distribution functions $n(\tilde{\omega}) = n(\omega - \mu)$ in powers of fugacity $z = \exp(\beta\mu)$:

$$P_c = \frac{32\pi^2 a^2}{m^2} \sum_{a=1}^{\infty} \sum_{b=1}^{\infty} \sum_{c=1}^{\infty} z^{a+b+c} \times \int_{\mathbf{p}\mathbf{q}\mathbf{k}\mathbf{l}} \mathbf{P} \frac{e^{-a\beta q^2/2m} e^{-b\beta k^2/2m} e^{-c\beta l^2/2m}}{\omega_p + \omega_q - \omega_k - \omega_l} \times (2\pi)^3 \delta^{(3)}(\mathbf{p} + \mathbf{q} - \mathbf{k} - \mathbf{l}). \quad (\text{A13})$$

Rescaling all momenta by $\sqrt{\beta/m}$ to make them dimensionless gives

$$P_c = \frac{8a^2 T}{\lambda^5} \sum_{a=1}^{\infty} \sum_{b=1}^{\infty} \sum_{c=1}^{\infty} z^{a+b+c} I_{abc}, \quad (\text{A14})$$

$$I_{abc} \equiv (2\pi)^{9/2} \int_{\mathbf{p}\mathbf{q}\mathbf{k}\mathbf{l}} \mathbf{P} \frac{e^{-aq^2/2} e^{-bk^2/2} e^{-cl^2/2}}{\frac{1}{2}(p^2 + q^2 - k^2 - l^2)} (2\pi)^3 \times \delta^{(3)}(\mathbf{p} + \mathbf{q} - \mathbf{k} - \mathbf{l}). \quad (\text{A15})$$

For the sake of justifying later manipulations, it is convenient to introduce a redundant $\exp(-0^+ p^2)$ convergence factor into the integral defining I_{abc} . We will evaluate I_{abc} by representing the energy denominator and the δ function as integrals of exponentials. Using the infinitesimal version (4.23) of the principal part prescription, we write

$$I_{abc} = (2\pi)^{9/2} \text{Re} \int_{\mathbf{p}\mathbf{q}\mathbf{k}\mathbf{l}} e^{-0^+ p^2} e^{-aq^2/2} e^{-bk^2/2} e^{-cl^2/2} \times \int_0^{i\infty} d\lambda e^{-(p^2 + q^2 - k^2 - l^2 - i0^+)\lambda/2} \int d^3 x e^{i\mathbf{x} \cdot (\mathbf{p} + \mathbf{q} - \mathbf{k} - \mathbf{l})}. \quad (\text{A16})$$

The \mathbf{p} , \mathbf{q} , \mathbf{k} , and \mathbf{l} integrations are now simple Gaussian integrals, yielding

$$I_{abc} = (2\pi)^{-3/2} \text{Re} \int_0^{i\infty} d\lambda e^{i0^+ \lambda} \int d^3 x (0^+ + \lambda)^{-3/2} \times (a + \lambda)^{-3/2} (b - \lambda)^{-3/2} (c - \lambda)^{-3/2} \times \exp\left[-\frac{x^2}{2} \left(\frac{1}{0^+ + \lambda} + \frac{1}{a + \lambda} + \frac{1}{b - \lambda} + \frac{1}{c - \lambda}\right)\right]. \quad (\text{A17})$$

The $\exp(i0^+ \lambda)$ prescription is now redundant and can be dropped. It's also convenient to change integration variables from λ to $\lambda + 0^+$ in order to remove the remaining 0^+ prescription from the integrand (noting that $a, b, c \neq 0$). The \mathbf{x} integral is Gaussian and yields

$$I_{abc} = \text{Re} \int_{0^+}^{i\infty+0^+} d\lambda [abc + 2bc\lambda - (a+b+c)\lambda^2]^{-3/2}. \quad (\text{A18})$$

The final integral is straightforward and gives

$$I_{abc} = \frac{1}{(a+b)(a+c)(abc)^{1/2}}. \quad (\text{A19})$$

The final result for this contribution to the pressure is

$$P_c = \frac{8a^2 T}{\lambda^5} \sum_{a=1}^{\infty} \sum_{b=1}^{\infty} \sum_{c=1}^{\infty} \frac{z^{a+b+c}}{(a+b)(a+c)(abc)^{1/2}}. \quad (\text{A20})$$

2. The three-circle diagram

The other second-order diagram, Fig. 1(b), is trivial in comparison. It's contribution to the pressure is

$$P_b = \frac{1}{2} \left(\frac{-8\pi a}{m} \right)^2 \oint_P \frac{1}{(ip_0 + \tilde{\omega}_p)^2} \left(\oint_Q \frac{1}{iq_0 + \tilde{\omega}_q} \right)^2. \quad (\text{A21})$$

One of the summation integrals is

$$\begin{aligned} \oint_Q \frac{1}{iq_0 + \tilde{\omega}_q} &= \int_{\mathbf{q}} [n(\tilde{\omega}_q) + \tfrac{1}{2}] = \int_{\mathbf{q}} n(\tilde{\omega}_q) \\ &= \left(\frac{m}{2\pi\beta} \right)^{3/2} \text{Li}_{3/2}(z). \end{aligned} \quad (\text{A22})$$

The other is easily obtained by differentiating with respect to μ :

$$\oint_P \frac{1}{(ip_0 + \tilde{\omega}_p)^2} = \beta \left(\frac{m}{2\pi\beta} \right)^{3/2} \text{Li}_{1/2}(z). \quad (\text{A23})$$

So,

$$P_b = \frac{8a^2 T}{\lambda^5} [\text{Li}_{3/2}(z)]^2 \text{Li}_{1/2}(z). \quad (\text{A24})$$

Putting P_b and P_c together gives the total second-order contribution to the pressure, which appears in Eq. (3.1). The first-order contribution of Fig. 1(a) is easily evaluated in a similar manner.

APPENDIX B: SMALL $\bar{\mu}$ EXPANSION OF N

1. The expansion

Consider the $(a/\lambda)^2$ term in the expansion (3.5) for N . First consider the term proportional to

$$\sum_{ijk} \frac{\bar{z}^{i+j+k}}{(ij)^{3/2} k^{1/2} (i+j+k)^{1/2}}. \quad (\text{B1})$$

Because of the explicit factor of a^2 , one might naively think one could use the order a^0 result $\bar{z} \approx 1$ for \bar{z} . But this would give

$$\sum_{ijk} \frac{1}{(ij)^{3/2} k^{1/2} (i+j+k)^{1/2}}, \quad (\text{B2})$$

which has logarithmic divergencies associated with $k \rightarrow \infty$, with i and j fixed. We can isolate these divergencies by re-writing the original sum as

$$\begin{aligned} \sum_{ijk} \frac{\bar{z}^{i+j+k}}{(ij)^{3/2} k^{1/2} (i+j+k)^{1/2}} &= \sum_{ijk} \left[\frac{\bar{z}^{i+j+k}}{(ij)^{3/2} k^{1/2} (i+j+k)^{1/2}} \right. \\ &\quad \left. - \frac{\bar{z}^k}{(ij)^{3/2} k} \right] + \sum_{ijk} \frac{\bar{z}^k}{(ij)^{3/2} k}. \end{aligned} \quad (\text{B3})$$

We can now safely set \bar{z} to 1 in the first sum on the left-hand side. The second sum is easy, giving $-\zeta(\frac{3}{2})^2 \ln(1-\bar{z})$. The small $\bar{\mu}$ result is then

$$\begin{aligned} \sum_{ijk} \frac{\bar{z}^{i+j+k}}{(ij)^{3/2} k^{1/2} (i+j+k)^{1/2}} &= \sum_{ijk} \left[\frac{1}{(ij)^{3/2} k^{1/2} (i+j+k)^{1/2}} \right. \\ &\quad \left. - \frac{1}{(ij)^{3/2} k} \right] - \zeta(\tfrac{3}{2})^2 \ln(-\beta\bar{\mu}) \\ &\quad + O(\bar{\mu}). \end{aligned} \quad (\text{B4})$$

The sum associated with the a/λ term of Eq. (3.5) must be expanded to first order in $\bar{\mu}$, where it suffers a similar problem. Naively,

$$\begin{aligned} \sum_{ij} \frac{\bar{z}^{i+j}}{(ij)^{3/2} (i+j)^{1/2}} &= \sum_{ij} \frac{1}{(ij)^{3/2} (i+j)^{1/2}} - \beta\bar{\mu} \sum_{ij} \frac{(i+j)^{1/2}}{(ij)^{3/2}} \\ &\quad + \dots \end{aligned} \quad (\text{B5})$$

The second term has logarithmic divergencies associated with (i) $i \rightarrow \infty$ with j fixed, and, symmetrically (ii) $j \rightarrow \infty$ with i fixed. Proceeding as before, we can isolate the divergent behavior by writing

$$\begin{aligned} \sum_{ij} \frac{\bar{z}^{i+j}}{(ij)^{3/2} (i+j)^{1/2}} &= \sum_{ij} \left[\frac{\bar{z}^{i+j}}{(ij)^{3/2} (i+j)^{1/2}} - \frac{\bar{z}^i}{i^2 j^{3/2}} - \frac{\bar{z}^j}{i^{3/2} j^2} \right] \\ &\quad + \sum_{ij} \left[\frac{\bar{z}^i}{i^2 j^{3/2}} + \frac{\bar{z}^j}{i^{3/2} j^2} \right]. \end{aligned} \quad (\text{B6})$$

In the first sum, we can now safely replace \bar{z} by $1 + \beta\bar{\mu}$ + $O(\bar{\mu}^2)$, and the second sum gives

$$\begin{aligned} 2\zeta(\tfrac{3}{2}) \text{Li}_2(\bar{z}) &= 2\zeta(\tfrac{3}{2}) \{ \zeta(2) + [-\ln(-\beta\bar{\mu}) + 1] \beta\bar{\mu} \} \\ &\quad + O(\bar{\mu}^2). \end{aligned} \quad (\text{B7})$$

The final result for the expansion is then

$$\begin{aligned} \sum_{ij} \frac{\bar{z}^{i+j}}{(ij)^{3/2}(i+j)^{1/2}} &= \sum_{ij} \frac{1}{(ij)^{3/2}(i+j)^{1/2}} + 2\zeta\left(\frac{3}{2}\right)\beta\bar{\mu} \\ &\times [-\ln(-\beta\bar{\mu}) + 1] \\ &+ \beta\bar{\mu} \sum_{ij} \frac{(i+j)^{1/2} - i^{1/2} - j^{1/2}}{(ij)^{3/2}} + O(\bar{\mu}^2). \end{aligned} \quad (\text{B8})$$

The last thing we need is the expansion of the sum in the order a^0 term of Eq. (1.5), which is just

$$\begin{aligned} \text{Li}_3(\bar{z}) &= \zeta(3) + \zeta(2)\beta\bar{\mu} + \frac{1}{2}[-\ln(-\beta\bar{\mu}) + \frac{3}{2}](\beta\bar{\mu})^2 \\ &+ O(\bar{\mu}^3). \end{aligned} \quad (\text{B9})$$

Combining the expansions (B4), (B8), and (B9) of the sums with the expansion (3.5) of N , we obtain

$$\begin{aligned} N &= \left(\frac{k_B T}{\hbar \omega_{\text{ho}}}\right)^3 \left\{ \zeta(3) + \left[\zeta(2)\beta\bar{\mu} - \frac{2a}{\lambda} \sum_{ij} \frac{1}{i^{3/2}j^{3/2}(i+j)^{1/2}} \right] + \left[\frac{3}{4}(\beta\bar{\mu})^2 - \frac{2a}{\lambda} \beta\bar{\mu} \sum_{ij} \frac{(i+j)^{1/2} - i^{1/2} - j^{1/2}}{i^{3/2}j^{3/2}} - \frac{4a}{\lambda} \beta\bar{\mu} \zeta\left(\frac{3}{2}\right) \right. \right. \\ &+ 8\left(\frac{a}{\lambda}\right)^2 \sum_{ijk} \frac{1}{(ij)^{3/2}k^{1/2}} \left(\frac{1}{(i+j+k)^{1/2}} + \frac{ij}{(i+k)(j+k)(i+j+k)^{1/2}} - \frac{1}{k^{1/2}} \right) \left. \left. - \frac{1}{2} \left(\beta\bar{\mu} - \frac{4a}{\lambda} \zeta\left(\frac{3}{2}\right) \right)^2 \ln(-\beta\bar{\mu}) \right. \right. \\ &\left. \left. + O\left(\frac{a}{\lambda}, \beta\bar{\mu}\right)^3 \right\}. \end{aligned} \quad (\text{B10})$$

If we now use the expansion (3.7) of $\bar{\mu}_c$, we obtain the result (3.9) presented in the main text.

2. Cancellation of logarithms

To understand the origins of the logarithms in the preceding analysis, consider a straight, naive, perturbative expansion in $\bar{\mu}$. Treating the $-\bar{\mu}\psi^*\psi$ term of the Lagrangian as a perturbation, the logarithms then arise from the diagrams of Fig. 14. Each diagram should be understood as evaluated at fixed \mathbf{x} , with effective chemical potential $\mu = \bar{\mu} - V(\mathbf{x})$, and then the result of the diagram integrated over \mathbf{x} . $\bar{\mu}$ is treated perturbatively, while $V(\mathbf{x})$ is not. The imaginary-time propagators in this perturbation theory, derived from the action (2.3), are

$$G_0(p_0, \mathbf{p}) = \frac{1}{ip_0 + p^2/2m + V(\mathbf{x})}, \quad (\text{B11})$$

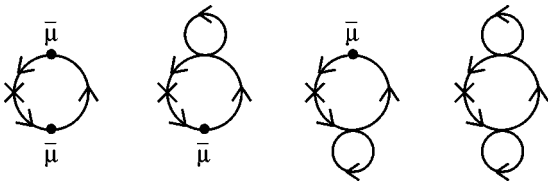


FIG. 14. Diagrams producing the infrared logarithm in the small $\bar{\mu}$ expansion of N . Each diagram should be understood as being evaluated with an effective chemical potential $\mu = \bar{\mu} - V(\mathbf{x})$ with $\bar{\mu}$ treated perturbatively. The dots represent the two-point vertex coming from treating the $-\bar{\mu}\psi^*\psi$ term in the Lagrangian perturbatively. The crosses are as in Fig. 2.

where we now set $\hbar = 1$ for convenience. The logarithms are produced by the infrared behavior, near the center of the trap, of the loops drawn large in the figure. Specifically, it is the $p_0=0, \mathbf{p}\rightarrow 0, \mathbf{x}\rightarrow 0$ behavior of these diagrams, where p is the loop momentum of those loops. The small loops are UV dominated and so, to this order in the expansion in a , are insensitive to \mathbf{x} near the center of the trap. The infrared divergencies due to the large loops then produce the same common factor for all diagrams:

$$\int d^3x \int d^3p [G(0, \mathbf{p})]^3 \propto \int \frac{d^6q}{q^6} = \text{log divergent}, \quad (\text{B12})$$

where we've introduced the six-dimensional phase-space vector

$$\mathbf{q} = \left(\frac{p_x}{\sqrt{2m}}, \frac{p_y}{\sqrt{2m}}, \frac{p_z}{\sqrt{2m}}, \sqrt{\frac{m}{2}}\omega_x x, \sqrt{\frac{m}{2}}\omega_y y, \sqrt{\frac{m}{2}}\omega_z z \right). \quad (\text{B13})$$

The cancellation of these logarithms at the phase transition occurs because, at the phase transition, the inverse susceptibility vanishes at the center of the trap. This condition is shown diagrammatically in Fig. 7, which implies that the logarithms generated by the diagrams of Fig. 14 cancel each other at the order of a under consideration.

APPENDIX C: NUMERICAL RESULTS FOR SUMS

The following sums were computed numerically using the iterative application of the Euler-MacLaurin formula.

$$\sum \frac{1}{i^{3/2}j^{3/2}(i+j)^{1/2}} \approx 2.416\,942\,200, \quad (\text{C1})$$

$$\sum_{ij} \frac{(i+j)^{1/2} - i^{1/2} - j^{1/2}}{i^{3/2}j^{3/2}} \approx -8.215\,157\,561, \quad (\text{C2})$$

$$\sum_{ijk} \frac{1}{(ijk)^{1/2}(i+k)(j+k)(i+j+k)^{1/2}} \approx 2.2111, \quad (\text{C3})$$

$$\sum_{ijk} \frac{1}{(ij)^{3/2}k^{1/2}} \left(\frac{1}{(i+j+k)^{1/2}} - \frac{1}{k^{1/2}} \right) \approx -16.70. \quad (\text{C4})$$

APPENDIX D: DERIVATION OF THE SUNSET DIAGRAM

Using the methods outlined in Appendix A, we will now reduce the sunset diagram (4.21) to the integral representation (4.22) in terms of distribution functions. Starting with

$$\begin{aligned} \Pi_{\psi}^{(d)}(0) = & -\frac{1}{2} \left(\frac{8\pi a}{m} \right)^2 \\ & \times \sum_{QKL} \frac{\beta \delta_{l_0 - q_0 - k_0} (2\pi)^d \delta^{(d)}(\mathbf{1} - \mathbf{q} - \mathbf{k})}{(il_0 + \omega_l)(iq_0 + \omega_q)(ik_0 + \omega_k)}, \end{aligned} \quad (\text{D1})$$

and rewriting the Kronecker δ function in (D1) as in Appendix A, we obtain

$$\begin{aligned} \Pi_{\psi}^{(d)}(0) = & -\frac{1}{2} \left(\frac{8\pi a}{m} \right)^2 \int_0^\beta d\alpha \sum_L \frac{e^{-i\alpha l_0}}{il_0 + \omega_p} \sum_Q \frac{e^{+i\alpha q_0}}{iq_0 + \omega_q} \\ & \times \sum_K \frac{e^{+i\alpha k_0}}{ik_0 + \omega_k} (2\pi)^d \delta^{(d)}(\mathbf{1} - \mathbf{q} - \mathbf{k}). \end{aligned} \quad (\text{D2})$$

Using the frequency sums (A4) and then performing the α integration,

$$\begin{aligned} \Pi_{\psi}^{(d)}(0) = & -\frac{1}{2} \left(\frac{8\pi a}{m} \right)^2 \int_{\mathbf{qkl}} n(\omega_l) n(\omega_q) n(\omega_k) \\ & \times \frac{e^{\beta\omega_l} - e^{\beta(\omega_q + \omega_k)}}{\omega_l - \omega_q - \omega_k} (2\pi)^d \delta^{(d)}(\mathbf{1} - \mathbf{q} - \mathbf{k}). \end{aligned} \quad (\text{D3})$$

The integrand is well behaved at $\omega_l = \omega_q + \omega_k$ (except for the infrared divergence where l , q , and k all go to zero, which is dealt with in the main text). However, as in Appendix A, it is convenient to introduce a spurious principal part prescription at this stage. Then, using Eq. (A6) and permuting integration variables, one arrives at Eq. (4.22).

The last term in Eq. (4.22), involving just one n , is proportional to

$$\int_{\mathbf{qkl}} \text{P} \frac{n(\omega_l)}{\omega_l - \omega_q - \omega_k} (2\pi)^d \delta^{(d)}(\mathbf{1} - \mathbf{q} - \mathbf{k}). \quad (\text{D4})$$

The \mathbf{qk} part of this integration is just a special case of Eq. (A11) with the momentum labels changed and \mathbf{p} set to zero. As described in Appendix A, it therefore gives zero contribution in dimensional regularization for $d=3$.

-
- [1] F. Dalfovo, S. Giorgini, L. P. Pitaevskii, and S. Stringari, *Rev. Mod. Phys.* **71**, 463 (1999).
- [2] S. Giorgini, L. P. Pitaevskii, and S. Stringari, *Phys. Rev. A* **54**, R4633 (1996).
- [3] M. Holzmann, G. Baym, and F. Laloë, *Phys. Rev. Lett.* (to be published).
- [4] P. Arnold, G. Moore, and B. Tomášik, e-print cond-mat/0107124.
- [5] V. A. Kashurnikov, N. Prokofev, and B. Svistunov, *Phys. Rev. Lett.* (to be published).
- [6] P. Arnold and G. Moore, *Phys. Rev. Lett.* **87**, 120401 (2001).
- [7] P. Arnold and G. Moore, *Phys. Rev. E* (to be published).
- [8] H. T. C. Stoof, *Phys. Rev. A* **45**, 8398 (1982); M. Bijlsma and H. T. C. Stoof, *ibid.* **54**, 5085 (1996).
- [9] P. Grüter, D. Ceperley, and F. Laloë, *Phys. Rev. Lett.* **79**, 3549 (1997).
- [10] M. Holzmann, P. Grüter, and F. Laloë, *Eur. Phys. J. B* **10**, 739 (1999).
- [11] M. Holzmann and W. Krauth, *Phys. Rev. Lett.* **83**, 2687 (1999).
- [12] G. Baym, J.-P. Blaizot, M. Holzmann, F. Laloë, and D. Vautherin, *Phys. Rev. Lett.* **83**, 1703 (1999).
- [13] G. Baym, J.-P. Blaizot, and J. Zinn-Justin, *Europhys. Lett.* **49**, 150 (2000).
- [14] P. Arnold and B. Tomášik, *Phys. Rev. A* **62**, 063604 (2000).
- [15] K. Huang, C. N. Yang, and J. M. Luttinger, *Phys. Rev.* **105**, 776 (1957).
- [16] K. Huang and C. N. Yang, *Phys. Rev.* **105**, 767 (1957).
- [17] E. Braaten and A. Nieto, *Eur. Phys. J. B* **11**, 143 (1999).
- [18] K. Huang, *Phys. Rev. Lett.* **83**, 3770 (1999).
- [19] K. Symanzik, *Nucl. Phys.* **B226**, 198 (1983); **B226**, 205 (1983).
- [20] See, for example, E. Braaten and A. Nieto, *Phys. Rev. B* **56**, 14745 (1997).
- [21] W. E. Caswell and G. P. Lepage, *Phys. Lett.* **167B**, 437 (1986); T. Kinoshita and G. P. Lepage, in *Quantum Electrodynamics*, edited by T. Kinoshita (World Scientific, Singapore, 1990).
- [22] See, for example, A. Manohar and M. Wise, *Heavy Quark Physics* (Cambridge University, New York, 2000); B. Grinstein, in *High Energy Phenomenology, Proceedings of the Workshop*, edited by R. Huerta and M. Perez (World Scientific, Singapore, 1992).
- [23] E. Braaten and A. Nieto, *Phys. Rev. D* **51**, 6990 (1995); **53**, 3421 (1996).
- [24] L. Brown and L. Yaffe, *Phys. Rep.* **340**, 1 (2001).
- [25] H. Georgi, *Annu. Rev. Nucl. Part. Sci.* **43**, 209 (1993); A. Manohar, in *Quarks and Colliders: Proceedings* (World Scien-

- tific, Singapore,1996); e-print hep-ph/9508245; D. Kaplan, *Effective Field Theories* (unpublished); e-print nucl-th/9506035.
- [26] A. Fetter and J. Walecka, *Quantum Theory of Many-Particle Systems* (McGraw Hill, New York, 1971).
- [27] C. Ford, I. Jack, and D. R. T. Jones, Nucl. Phys. **B387**, 373 (1992); **B504**, 551(E) (1997).
- [28] K. Farakos, K. Kajantie, K. Rummukainen, and M. Shaposhnikov, Nucl. Phys. **B425**, 67 (1994).
- [29] E. Braaten, H.-W. Hammer, and S. Hermans, e-print cond-mat/0012043.
- [30] M. Luban, Phys. Rev. **128**, 965 (1962); see also Sec. 28 of Ref. [26].
- [31] S. Grossman and M. Holthaus, Z. Naturforsch. A **50**, 921 (1955); Phys. Lett. A **208**, 188 (1995); W. Ketterle and N. J. van Druten, Phys. Rev. A **54**, 656 (1996); K. Kirsten and D. J. Toms, *ibid.* **54**, 4188 (1996).
- [32] J. R. Ensher, D. S. Jin, M. R. Matthews, C. E. Wieman, and E. A. Cornell, Phys. Rev. Lett. **77**, 4984 (1996).
- [33] P. S. Julienne, F. H. Mies, E. Tiesinga, and C. J. Williams, Phys. Rev. Lett. **78**, 1880 (1997).
- [34] H. M. J. M. Boesten, C. C. Tsai, J. R. Gardner, D. J. Heinzen, and B. J. Verhaar, Phys. Rev. A **55**, 636 (1997).
- [35] J. Kapusta, *Finite-Temperature Field Theory* (Cambridge University, New York, 1989).